Differential Activation of Partially Redundant Δ9 Stearoyl-ACP Desaturase Genes Is Critical for Omega-9 Monounsaturated Fatty Acid Biosynthesis During Seed Development in Arabidopsis. — Source link ⧉

Sami Kazaz, Guillaume Barthole, Frédéric Domergue, Frédéric Domergue ...+7 more authors

Institutions: Université Paris-Saclay, University of Bordeaux, Centre national de la recherche scientifique

Topics: Arabidopsis, Oleic acid, Fatty acid, Endosperm and Arabidopsis thaliana

Related papers:

- WRINKLED1 specifies the regulatory action of LEAFY COTYLEDON2 towards fatty acid metabolism during seed maturation in Arabidopsis

- Transcriptional Activation of Two Delta-9 Palmitoyl-ACP Desaturase Genes by MYB115 and MYB118 Is Critical for Biosynthesis of Omega-7 Monounsaturated Fatty Acids in the Endosperm of Arabidopsis Seeds

- The biochemical characterization of a high-stearic acid sunflower mutant reveals the coordinated regulation of stearoyl-acyl carrier protein desaturases.

- Overexpression of Acyl-ACP Thioesterases, CpFatB4 and CpFatB5, Induce Distinct Gene Expression Reprogramming in Developing Seeds of Brassica napus

- The Arabidopsis stearoyl-acyl carrier protein-desaturase family and the contribution of leaf isoforms to oleic acid synthesis.

Share this paper:

Differential Activation of Partially Redundant Δ9 Stearoyl-ACP Desaturase Genes Is Critical for Omega-9 Monounsaturated Fatty Acid Biosynthesis During Seed Development in Arabidopsis

Sami Kazaz, Guillaume Barthole, Frédéric Domergue, Hasna Ettaki, Alexandra To, Damien Vasselon, Delphine de Vos, Katia Belcram, Loic Lepiniec, Sébastien Baud

Differential Activation of Partially Redundant Δ9 Stearoyl-ACP Desaturase Genes Is Critical for Omega-9 Monounsaturated Fatty Acid Biosynthesis During Seed Development in Arabidopsis

Sami Kazaz[a], Guillaume Barthole[a], Frédéric Domergue[b,c], Hasna Ettaki[a], Alexandra To[a], Damien Vasselon[a], Delphine De Vos[a], Katia Belcram[a], Loïc Lepiniec[a], and Sébastien Baud[a]

[a]Institut Jean-Pierre Bourgin, INRAE, CNRS, AgroParisTech, Université Paris-Saclay, 78000 Versailles, France

[b]Université de Bordeaux, Laboratoire de Biogenèse Membranaire, UMR 5200, Villenave d'Ornon, France

[c]CNRS, Laboratoire de Biogenèse Membranaire, UMR 5200, Villenave d'Ornon, France

Running title

Roles of Δ9 stearoyl-ACP desaturases in seeds

Corresponding author e-mail

sebastien.baud@inrae.fr

One sentence summary

Oleic acid and derivatives synthesized by four Δ9 stearoyl-ACP desaturases, FAB2, AAD1, AAD5, and AAD6, play critical roles during Arabidopsis embryo development and seed maturation.

The author responsible for distribution of materials integral to the findings presented in this article in accordance with the policy described in the Instructions for Authors (www.plantcell.org) is: Sébastien Baud (sebastien.baud@inrae.fr). Contact information: Institut Jean-Pierre Bourgin, UMR1318 INRA-AgroParisTech, INRA Centre de Versailles-Grignon, Route de Saint-Cyr (RD10), 78026 Versailles Cedex, France. Tel. +33 1 30 83 33 25

ABSTRACT

The spatiotemporal pattern of deposition, final amount, and relative abundance of oleic acid (*cis*-ω-9 C18:1) and its derivatives in the different lipid fractions of seeds suggested a preeminent role of Δ9 stearoyl-ACP desaturases (SADs) during seed development. Accordingly, four SAD-coding genes (*FAB2, AAD5, AAD1*, and *AAD6*) are transcriptionally induced in this organ. The three most highly expressed ones are directly activated by the WRINKLED1 transcription factor. The thorough characterization of a collection of 30 simple, double, triple, and quadruple mutants affected in SAD-coding genes then revealed major roles played by these desaturases at various stages of seed development. First, production of oleic acid by FAB2 and AAD5 appears to be critical at the onset of embryo morphogenesis. Double homozygous plants from crossing *fab2* and *aad5* could never be obtained, and further investigations revealed that the double mutation resulted in the arrest of embryo development before the globular stage. During later stages, these two SADs, together with AAD1, participate in the elaboration of the embryonic cuticle, a barrier essential for embryo-endosperm separation during the phase of invasive embryo growth through the endosperm. This study finally demonstrates that the four desaturases redundantly contribute to storage lipid production during the maturation phase.

INTRODUCTION

In spermatophyta, seed production interrupts the life cycle and allows survival and dispersion of plants (Bewley, 1997). To establish the next generation, seeds package together genetic material from the species and nutrients essential to fuel post-germinative seedling establishment. In Angiosperms, seeds originate from the fertilized ovule: the double fertilization of the embryo sac initiates the development of two zygotes, the diploid embryo and the triploid endosperm. Several layers of maternal origin derived from the ovular integuments and referred to as the seed coat protect these zygotic tissues. The coordinated growth of these three tissues leads to the formation of seeds. This developmental process is classically divided into two main phases: embryo morphogenesis and maturation (Vicente-Carbajosa and Carbonero, 2005). The early morphogenetic phase of embryogenesis establishes the basic plant body organization of the embryo (Laux and Jürgens, 1997). The maturation phase which follows consists of the accumulation of reserve compounds and the preparation of the embryo for desiccation and dormancy (Baud et al., 2008). The maturation process is developmentally controlled by a complex network of transcription factors induced at the onset of this phase and named master regulators of seed maturation (Lepiniec et al., 2018).

Main seed reserves consist of storage proteins, carbohydrates, and storage lipids. Tissue localization and relative proportions of these compounds vary greatly depending on the species considered, but a source of nitrogen and a source of carbon are usually associated. Exalbuminous seeds of *Arabidopsis thaliana* accumulate seed storage proteins and triacylglycerols (TAGs) (Baud et al., 2002). The residual endosperm in mature *Arabidopsis* seeds consists in a thin peripheral cell layer. Reserves are massively stored in a central enlarged embryo structure. Beyond the strong imbalance observed between the amounts of reserves accumulated in the two zygotes, the composition of these reserves was also shown to be clearly different (Barthole et al., 2014). In the embryo, the vast majority of fatty acids (FAs) found in TAGs consist of oleic acid (*cis*-ω-9 C18:1) and its elongated and polyunsaturated derivatives, whereas the relative abundance of ω-7 monounsaturated FAs (MUFAs) is very low. All the FAs present in the embryo were also detected in the endosperm, but the latter contains much higher proportions of ω-

7 MUFAs, that represent more than 20 mol % of total FAs in this compartment (Penfield et al., 2004; Li et al., 2006). MYB115 and MYB118, two transcription factors of the MYB family induced in the endosperm at the onset of the maturation phase, were recently shown to control the amount and composition of the reserves stored in this tissue (Barthole et al., 2014; Troncoso-Ponce et al., 2016a).

In plants, *de novo* synthesis of FAs is localized in plastids and uses end products of the glycolysis as carbon source (Harwood, 1996; Troncoso-Ponce et al., 2016b). TAGs, which are formed from glycerol and FAs, are assembled within the endoplasmic reticulum (ER) and stored in dedicated structures, the oil bodies (Bates et al., 2013). Oil production, like other maturation-related programs, is controlled at the transcriptional level by the master regulators of seed maturation, either directly or indirectly depending on the target genes considered (Baud et al., 2007b; Baud and Lepiniec, 2010). A regulator of the APETALA2/ethylene-responsive element binding (AP2/EREBP) family induced by master regulators, named WRINKLED1 (WRI1), was shown to play a key role in the transcriptional activation of FA biosynthetic genes at the onset of the maturation phase (Cernac et al., 2004; Marchive et al., 2014). Upon binding to AW *cis*-regulatory elements present in the promoter sequences of these genes (Maeo et al., 2009), WRI1 recruits the Mediator complex and, in turn, the Pol II complex to initiate their transcription (Kim et al., 2016), thus promoting sustained rates of FA production.

Plastidial production of long-chain saturated FAs is performed in a stepwise manner by the type II FA synthase. Stromal soluble acyl-acyl carrier protein desaturases (AADs) can introduce a carbon-carbon double bond within these saturated acyl chains to form *cis*-MUFAs (Shanklin and Cahoon, 1998). Depending on their regio- and substrate specificity, AADs synthesize *cis*-MUFAs differing by the position of the double bond within their aliphatic chain. While Δ9 stearoyl-ACP desaturases (SADs) efficiently desaturate stearic acid (C18:0) to form oleic acid, Δ9 palmitoyl-ACP desaturases (PADs) prefer palmitic acid (C16:0) and mainly produce palmitoleic acid (*cis*-ω-7 C16:1) (Cahoon et al., 1998). In seeds of *Arabidopsis*, oleic acid can be elongated in the ER by the acyl-CoA elongase complex, yielding ω-9 very-long-chain MUFAs like gondoic acid (*cis*-ω-9 C20:1) and erucic acid (*cis*-ω-9 C22:1), or further desaturated by membrane-bound FA desaturases to form linoleic acid (C18:2) and α-linolenic acid (C18:3). Palmitolic acid is also efficiently elongated

4

to vaccenic acid (*cis*-ω-7 C18:1), then to paullinic acid (*cis*-ω-7 C20:1), but none of these ω-7 MUFAs are further desaturated.

The *Arabidopsis* genome codes for seven closely related AADs named FAB2/SSI2 and AAD1-6/SAD1-6 (Kachroo et al., 2007). The PADs catalyzing the biosynthesis of ω-7 MUFAs in maturing seeds have been unambiguously identified (Bryant et al., 2016). Transcriptional activation of *AAD2* and *AAD3* in the endosperm by MYB115 and MYB118 is critical for ω-7 MUFA accumulation in this compartment (Troncoso-Ponce et al., 2016a). Only traces of ω-7 MUFAs are detected in seeds of *aad2 aad3* double mutants. In contrast, the identity of the desaturase(s) responsible for the massive production of ω-9 MUFAs occurring in *Arabidopsis* seeds remains unclear. Only slight decreases in the proportions of oleic acid were measured in *fab2* and *aad5* mutant seeds, where the FA production capacity is not severely compromised (Lightner et al., 1997; Jin et al., 2017). These findings raised the question of a putative functional redundancy between FAB2, AAD5, and possibly other AAD isoforms in developing *Arabidopsis* seeds.

To identify the desaturases participating in ω-9 MUFA production in seeds, we thoroughly characterized the expression patterns of the seven *AADs* in seed tissues. Four candidates encoding SADs appeared to be expressed in zygotic tissues. We provide evidence that the expression of three of them is directly induced by WRI1. Then, we report the functional characterization of these candidates and we demonstrate that they play critical but partially redundant roles at different stages of seed development. *FAB2* and *AAD5*, the most highly expressed *SADs*, are essential during early embryo morphogenesis. The development of *aad5 fab2* double mutant embryos is arrested at an early globular stage. Later during embryo development, these two *SADs*, together with *AAD1*, play a key role during the phase of invasive embryo growth through the endosperm. This study finally reveals that FAB2, AAD1, AAD5, and AAD6 redundantly participate in oil storage during the maturation phase. Taken together, these results reveal the importance of the SADs during distinct and critical phases of seed development and underline the diverse uses made of ω-9 MUFAs for the elaboration of different classes of lipids in seeds.

RESULTS

Production and uses of ω-9 monoenes in seeds of *Arabidopsis*

Before addressing the role of SADs in seeds, we precisely characterized the accumulation patterns of ω-9 MUFAs and their derivatives in developing seeds. Wild-type seeds of the Columbia-0 (Col-0) accession were dissected from siliques during the course of development and their total FA content was analyzed by gas chromatography (GC). Oleic acid, its polyunsaturated (linoleic acid and α-linolenic acid) and very-long-chain MUFA derivatives (gondoic acid and erucic acid) were massively deposited between 8 and 15 days after anthesis (DAA) (Figure 1A). A slower accumulation rate was observed during late maturation. The amount of these FAs finally slightly declined during seed desiccation after the nutrient supply from the mother plant has definitively ceased. In mature dry seeds, ω-9 monoenes and their derivatives accounted for more than 80 % of total FAs.

To precisely identify the location of these FAs, mature seeds were then dissected prior to GC analysis. The two fractions obtained, embryos on one side, endosperms with seed coats attached on the other, were studied separately. Considering that seed integuments undergo programmed cell death during the maturation phase (Beeckman et al., 2000), the analysis of the second fraction reflected the sole endosperm content. In agreement with the differential partitioning of total FAs previously reported between zygotic tissues of *Arabidopsis* seeds (Li et al., 2006; Barthole et al., 2014), the total amount of ω-9 MUFAs and derivatives in the embryo was 10-times that of the endosperm (Figure 1B). While they accounted for more than 80 % of total FAs in the embryo, their relative proportion was 60 % of total FAs in the endosperm due to a specific and high accumulation of ω-7 MUFAs in this compartment (Bryant et al., 2016; Troncoso-Ponce et al., 2016a).

Finally, different classes of lipids were analyzed separately in mature dry seeds. Total lipids were first extracted from a batch of seeds and subjected to thin-layer chromatography to separate TAGs from polar lipids. Analyses of the two lipid fractions by GC revealed that ω-9 MUFAs and their derivatives accounted for 86 and 68 Mol % of total FAs in TAGs and polar lipids, respectively (Figure 1C). In parallel, a second batch of seeds was subjected to extensive delipidation, before analyzing by

6

GC-MS the residual bound lipids corresponding to the cuticular layers that are primarily produced by the seed coats. Analysis of the seed polyester composition revealed aliphatic monomers typical of suberin, with dicarboxylic and ω-hydroxy C18:1 and C18:2 FAs representing 28 Mol % of total monomers (Figure 1D).

The *AAD* genes are differentially expressed in seeds of *Arabidopsis*

We next examined the expression profiles of the seven *Arabidopsis* genes predicted to encode AADs in the search for seed-expressed candidates potentially contributing to the synthesis of ω-9 MUFAs in this organ. The expression pattern of the *AAD* genes in wild-type plants of the accession Col-0 was investigated by quantitative RT-PCR. A set of cDNA prepared from a range of plant organs (Supplemental Figure 1) and different stages of developing seeds was analyzed (Figure 2A). The results obtained confirmed the induction of *AAD2* and *AAD3*, two PAD-coding genes, in maturing seeds (Troncoso-Ponce et al., 2016a). They also revealed the ubiquitous accumulation patterns of *AAD1*, *AAD5*, *AAD6*, and *FAB2* transcripts. Interestingly, peaks of transcript accumulation were measured for these four *AADs* during seed maturation. As for *AAD4*, only traces of transcripts could be detected in the tissues analyzed. To further characterize the expression patterns of the seed-expressed *AADs*, maturing seeds aged 12 and 16 days after anthesis (DAA) were manually dissected prior to RNA extraction. Expression in the embryo on one side, and in the endosperm with seed coat attached on the other side, were then independently analyzed (Figure 2B). This procedure confirmed a preferential expression of *AAD2* and *AAD3* in the endosperm/seed coat fraction (Troncoso-Ponce et al., 2016a). On the contrary, *AAD1*, *AAD5*, and *FAB2* transcripts were detected at high levels in the two seed fractions analyzed. The relative abundance of these transcripts in embryos increased during the course of seed maturation. *AAD6* mRNA accumulation pattern was distinct from those of the above-mentioned groups: *AAD6* transcripts were detected in the two seed fractions analyzed, but their abundance was lower in 16-DAA embryos than in 12-DAA embryos.

To gain complementary information about the expression patterns of the *AADs*, we used the *Escherichia coli uidA* gene encoding ß-glucuronidase (GUS) as a reporter gene system (Figure 3). In transgenic *Arabidopsis* lines transformed with *ProAAD2:uidA* and *ProAAD3:uidA* constructs, GUS staining was observed in the

7

maturing endosperm, as previously described in Troncoso-Ponce et al. (2016a). A careful examination of the plant material prepared also revealed a localized activity of *ProAAD2* in stipules and an activity of *ProAAD3* in root tips (Supplemental Figure 2A-B). Analysis of *ProAAD6:uidA* plantlets grown *in vitro* revealed an intense GUS staining in roots and apical meristems. After transfer to soil, further characterization of these plants showed that cauline leaves, flowers, seed funiculi, and maturing embryos also exhibited GUS activity. Leaves and apical meristems of *in vitro* grown *ProAAD1:uidA* plantlets were stained. GUS activity was also detected in flowers, maturing embryos and endosperms of these lines. For these 4 *AAD* genes, GUS histochemical patterns observed with transcriptional *ProAAD:uidA* fusions were consistent with the patterns of mRNA accumulation (Figure 2 and Supplemental Figure 1). In contrast, important discrepancies were noted when comparing the GUS staining observed in *ProAAD5:uidA* and *ProFAB2:uidA* transgenic lines (Supplemental Figure 2C-E) with the patterns of *AAD5* and *FAB2* mRNA accumulation, respectively (Figure 2 and Supplemental Figure 1). For example, *AAD5* transcript levels were high in leaves while no GUS activity could be detected. Similarly, *FAB2* transcripts were very abundant in seeds whereas corresponding GUS staining was very weak. We therefore generated *ProAAD5:AAD5g:uidA* and *ProFAB2:FAB2g:uidA* lines to cope with the presence of putative *cis*-regulatory elements lying downstream of the translational start and with post-transcriptional regulations that could potentially confer higher mRNA stability to *AAD5* and *FAB2* mRNAs. Ubiquitous GUS staining was observed in *ProFAB2:FAB2g:uidA* lines while intense GUS activity could be detected in virtually every tissue of *ProAAD5:AAD5g:uidA* lines, with the exception of petals (Figure 3). This time, the GUS histochemical patterns obtained were fully consistent with the patterns of mRNA accumulation. Finally, a transcriptional *ProAAD4:uidA* fusion and a translational *ProAAD4:AAD4:uidA* fusion were prepared. These fusions were assayed for the resulting *uidA* expression pattern in transgenic lines but it was not possible to detect any GUS activity with either of the two constructs, in agreement with corresponding mRNA accumulation profile (Figure 2). Together, these data underlined the good correlation existing between ω-9 MUFA biosynthesis in seeds (Figure 1) and the expression profiles of four of the *AADs*, namely *AAD1*, *AAD5*, *AAD6*, and *FAB2*.

AAD1, AAD5, and AAD6, like FAB2, are stearoyl-ACP desaturases

The enzymatic function of FAB2 is well demonstrated (Lightner et al., 1994; Kachroo et al., 2001; Kachroo et al., 2007). The substrate-binding pocket of this Δ9 SAD is deep enough to accommodate C18:0, leading to the production of cis-ω-9 C18:1. The *Arabidopsis* AADs share a high degree of amino acid sequence similarity and a common structural fold (Kachroo et al., 2007). After alignment of these sequences, 3D structure modeling was performed thanks to the SWISS-MODEL server (http://swissmodel.expasy.org) (Bordoli et al., 2009; Arnold et al., 2006). The Δ9 SAD from *Ricinus communis* (PDB code 1AFR) was used as a template. This approach showed that the amino acid residues lining the bottom part of the substrate-binding pocket of AAD1, AAD5, and AAD6 are identical to the corresponding residues in the FAB2 and *R. communis* Δ9 SAD sequences, suggesting that the substrate-binding pockets of all these enzymes can accommodate C18:0 (Supplementary Figure 3). Accordingly, *in vitro* biochemical assays demonstrated that AAD1 and AAD5 utilize C18:0-ACP as a preferred substrate that they desaturate at position ω-9 (Kachroo et al., 2007).

In order to determine whether AAD1, AAD5, and AAD6 can contribute to ω-9 MUFA synthesis *in planta*, these isoforms were expressed in a *fab2* mutant background. The Δ9 PAD AAD2 was used as a negative control in this experiment. As previously reported (Lightner et al., 1994), leaves of the *fab2* mutant exhibited a modified FA composition, with considerably increased proportions of C18:0 compared to the wild type, and decreased levels of C16:3 (Figure 4). The mutant was stably transformed with $ProFAB2_{1kb}$:AADc constructs allowing efficient expression of the cDNAs under study in vegetative organs (Supplemental Figure 2E and Supplemental Figure 4). For each construct considered, three independent lines were analyzed. Rosette leaves of plants grown *in vitro* for 26 days were subjected to GC analysis. The levels of C18:0 appeared significantly reduced and that of C16:3 significantly increased in *fab2* transformed lines overexpressing *FAB2*, *AAD1*, *AAD5*, or *AAD6* compared with *fab2*. This effect was specific since overexpression of the Δ9 PAD-coding gene *AAD2* did not complement the mutant phenotype. The partial restoration of the wild-type FA composition obtained with *AAD1* and *AAD6* confirmed the results of similar approaches previously reported by Kachroo et al. (2007) and Klinkenberg et al. (2014), respectively. Although statistically significant, the partial phenotypic reversion observed with *AAD1*, *AAD5,* and *AAD6* was not as pronounced as the one obtained with *FAB2*. This may be related to the lower accumulation levels

of corresponding transcripts (Supplemental Figure 4), suggesting contrasted stabilities of the *AAD* transcripts. Another possible explanation may lie in the low specific activity of certain of the SAD isoforms with respect to FAB2 (Kachroo et al., 2007).

Impact of the *aad* mutations on ω-9 monoene accumulation in seeds

To further characterize the four SAD isoforms expressed in *Arabidopsis* seeds, a collection of *aad1*, *aad5*, *aad6*, and *fab2* T-DNA insertion alleles (all in Col-0 background) was obtained and characterized at the molecular level (Figure 5A-B). Considering that functionally redundant co-expressed isoforms may hamper this approach of reverse genetics, multiple mutants were created. Double mutants were first generated by crossing homozygous single mutants: *aad1 fab2* and *aad6 fab2* double mutants were thus generated. After several rounds of screening, we could get *aad5 fab2*/+ and *aad5*/+ *fab2* plants homozygous at one locus and heterozygous at the other, but no *aad5 fab2* double homozygous mutants. Moreover, whereas vegetative development of *aad5 fab2*/+ plants appeared similar to that of the wild type, *aad5*/+ *fab2* plants exhibited a dwarf phenotype *in vitro* and rapidly died when transplanted into soil in the greenhouse (Supplementary Figure 5). To overcome this limitation, additional leaky *aad5* and *fab2* mutations resulting from T-DNA insertions in the promoter sequences of *AAD5* or *FAB2* were selected and named *aad5-1* and *fab2-1*. Accumulation levels of *AAD5* or *FAB2* transcripts appeared to be significantly decreased in maturing seeds of *aad5-1* and *fab2-1* mutants, respectively (Figure 5C and D). It was possible to obtain *aad5 fab2* double homozygous mutants by combining a knockout mutation in one gene with a leaky mutation in the other. Triple and quadruple mutants were next generated and the resulting collection of 30 mutant genotypes was grown under controlled conditions before mature dry seeds were subjected to GC analysis (Figure 5E). The *aad* mutations tested exhibited additive effects and contributed to increasing the proportions of C18:0 and their elongated derivatives (C20:0 and C22:0) while concomitantly decreasing the levels of ω-9 MUFAs and their derivatives. The most severe phenotypes were observed in seeds of the quadruple mutants, with saturated FAs representing nearly half of the total FAs while they accounted for less than 6 Mol % in the Col-0 background. These data established the redundant roles played by AAD1, AAD5, AAD6, and FAB2 in the production of ω-9 MUFAs in seeds. What is more, a careful examination of the seed

FA compositions of the 30 genotypes supported the idea that the respective contributions of the different SADs to the production of ω-9 MUFAs in seeds were roughly proportional to their expression levels. Seeds from two severely affected genotypes were then dissected prior to GC analyses (Supplementary Figure 6). The two seed fractions examined exhibited similar FA compositional changes.

To further evaluate the impact of these mutations on lipid homeostasis, the FA composition of different classes of lipids was next determined for a subset of mutant lines (Supplementary Figure 7). Major changes in the FA composition of TAGs were measured that faithfully reflected the overall compositional changes previously observed at the total FA level (Figure 5E). Though significant, the compositional remodeling of polar lipids and surface lipid polyesters was more attenuated. Interestingly, the relative proportions of PUFAs and derivatives in these different lipid fractions appeared rather stable in comparison with the reported drops in ω-9 MUFA contents, as if the monoenes were used as an adjustment variable.

FAB2 and AAD5 play redundant roles during early embryogenesis

FAB2 and *AAD5* are on two different chromosomes. These nonlinked genes therefore segregate randomly when forming female and male gametophytes. Dissected siliques from *aad5 fab2*/+ plants contained approximately one quarter of seeds exhibiting a severe shrunken phenotype, suggesting that embryogenesis of double homozygous mutant embryos might be arrested (Figure 6A-B). Consistent with this hypothesis, genotyping the progeny of self-fertilized *aad5 fab2*/+ plants confirmed the lack of double homozygous mutants while showing a 2:1 ratio of heterozygous to wild-type plants for the segregating mutant allele (Figure 6C).

Reciprocal crosses between wild-type and *aad5 fab2*/+ plants were also performed. Genotyping of the offspring population showed that the *aad5 fab2* genotype could be transmitted by gametes with the same efficiency as the *aad5 FAB2* and *AAD5 fab2* genotypes (Supplemental Figure 8A-B). In agreement with this, histological analysis of mature pollen grains by Alexander's stain solution revealed that all pollen grains were pink and therefore viable in all the genotypes tested (Supplemental Figure 8C). In parallel, observation of unfertilized ovules within carpels of the three genotypes considered failed to reveal any aborted ovule (Supplemental Figure 8D). Together, these data showed that the impossibility to get *aad5 fab2* double homozygous mutants could not be attributable to abnormalities or

11

altered viability of *aad5 fab2* gametes. Instead, these data reinforced the hypothesis of the embryo lethality of the *aad5 fab2* double mutants.

We therefore examined the morphogenesis of *aad5 fab2* embryos. As a first approach, early seed development was monitored by differential interference contrast (DIC) microscopy (Figure 6D). The development of mutant embryos was found to stop before the globular stage. To precisely determine the stage of embryo morphogenesis during which the *aad5 fab2* mutations arrest growth, we conducted a detailed examination of early developing seeds by confocal microscopy (Figure 6E). The material was stained with calcofluor, a non-specific fluorochrome that binds with cellulose in the cell walls, to allow examining cell organization in the embryos. Although the staining of cell walls appeared less intense in *aad5 fab2* embryos than in wild-type embryos, it was always possible to identify a suspensor and an embryo proper in the mutant background, suggesting that the first asymmetric division of the zygote was not affected. Further development of the embryo proper was impaired, with a majority of embryos arrested at the 1- to 2-cell stage. Within embryo cells, stained material possibly corresponding to cell plates was frequently observed, revealing interrupted cell divisions. Embryos arrested after the 8-cell stage were infrequently observed and they displayed aberrant positioning of the division planes.

To confirm that the embryo lethal phenotype was due to the T-DNA insertions in the *AAD5* and *FAB2* genes, we finally rescued the *aad5 fab2* double mutant with constructs encompassing either *AAD5* or *FAB2* gene. For this purpose, *aad5-2 fab2-3*/+ plants were transformed with the *ProFAB2:FAB2g* or *ProAAD5:AAD5g* construct and *aad5-2 fab2-3* double mutants could be recovered (Supplemental Figure 9 and Supplemental Figure 10). The leaf FA composition of double mutants rescued by the constructs was investigated by GC (Supplemental Figure 10C). The FA composition of mutants rescued with the *ProFAB2:FAB2g* construct was close to that of the wild type whereas the proportion of C18:0 in leaves of the plants transformed with the *ProAAD5:AAD5g* construct fell between that of *fab2* and the wild type. Taken together, these data indicate that AAD5 and FAB2 have overlapping functions that are essential for early embryo morphogenesis.

AAD1, AAD5, and FAB2 play redundant roles in embryo-endosperm separation
After acquisition of bilateral symmetry at heart stage, the cotyledons arise from the flanks of the apical domain of the embryo. The early-maturing embryo elongates

invasively through the endosperm, which partially breaks down. Physically constrained by the surrounding seed coat and persistent endosperm, the embryo then progresses from torpedo to upturned-U stage, yielding mature seeds shaped like prolate spheroids (Baud et al., 2002; Tsuwamoto et al., 2008; Moussu et al., 2017). After *aad1 fab2* and *aad5-1 fab2-2* double homozygous mutant plants were generated, observation of the progeny of these plants using a binocular magnifier revealed an unusual seed shape phenotype. Many seeds exhibited a twisted appearance (Figure 7A; Supplemental Figure 11A). The frequency of misshapen seeds was higher in the *aad1 fab2* background (50%) than in the *aad5-1 fab2-2* background (25%) (Figure 7D). Reciprocal crosses between wild-type and mutant plants were performed, and the absence of misshapen seeds among the offspring population established that the twisted phenotype was not of maternal origin (Supplemental Figure 11D). The external morphology of twisted seeds was further examined through scanning electron microscopy (SEM) (Figure 7B; Supplemental Figure 11B). Cells of the outermost seed coat layer exhibited normal characteristics. However, the reticulate pattern they produced appeared distorted by an abnormal folding of the embryo within the seed. In order to precisely assess embryo morphology in mature seeds, dry seeds were imbibed and embryos were excised before observations were realized through SEM (Figure 7C; Supplemental Figure 11C). This approach revealed a Z-folding of mutant embryos strikingly different from the upturned-U shape of their wild-type counterparts.

To determine when the mutations first affected embryo morphogenesis, developing seeds harvested at different stages were cleared and observed by DIC microscopy. Mutant embryos did not display any visible defect up to the heart stage (Figure 8A; Supplemental Figure 12A). At the torpedo stage, 8 DAA, double mutant embryos lost their bilateral symmetry because of an apparent adhesion of the cotyledon facing the integuments to surrounding tissues. Their overall morphology was conserved though. Within the next 48 h, mutant embryos then elongated in a looped structure that ultimately yielded Z-shaped mature embryos strongly adherent to the persistent endosperm.

Since the cuticular layer that surrounds the embryo is essential for embryo-endosperm separation and normal embryo growth and curvature (Xing et al., 2013; Fiume et al., 2016), we looked for any evidence of alteration in the cuticle in *aad1 fab2* and *aad5-1 fab2-2* double homozygous embryos. Defects in the cuticle are

frequently associated with an increased permeability to water-soluble molecules that can be monitored with toluidine blue uptake (Tanaka et al., 2004; Xing et al., 2013). We therefore performed qualitative toluidine blue permeability assays on cotyledons to test for cuticle integrity in mutant lines. Etiolated seedlings were first submerged in the hydrophilic dye, rinsed with water, and then observed with a binocular magnifier. In wild-type cotyledons, epidermal cells efficiently blocked dye uptake (Figure 8B; Supplemental Figure 12B). In contrast, the cotyledons of etiolated twisted mutants exhibited patches of blue staining, suggesting compromised cuticle function. Similar observations were made when the experiment was repeated with cotyledons of seedlings germinated in the light (Figure 8C; Supplemental Figure 12C).

Cotyledonary cuticle was directly observed through confocal scanning laser microscopy using the lipophilic fluorescent dye Auramine O reported to display a strong affinity for acidic and unsaturated waxes, as well as for cutin monomers (Buda et al., 2009; Fiume et al., 2016). On the surface of protodermal cells, a smooth and continuous cuticle layer could be observed in all the genotypes analyzed, ruling out the hypothesis of major structural alterations or interruptions of the cuticle layer as a cause for its compromised function (Supplemental Figure 13A). The content and composition of the cutin polymer on seedling cotyledons was then assessed by GC-MS. In agreement with microscopy observations, the total cutin load, as well as that of its major constituent C18:2 dicarboxylic FA, was barely affected in mutant cotyledons (Supplemental Figure 13B). However, significant changes were measured in the monomer composition of the lipid polyester (Figure 7E-G; Supplemental Figure 13C). In particular, a significant drop in C18:1 dicarboxylic FA was detected in the double mutants together with a concomitant increase in C18:0 and saturated VLCFA. Despite the limited proportions of the above-mentioned monomers in the cuticle layer, their imbalance seems to greatly affect the function of this hydrophobic barrier.

Reduced expression of *SAD* genes impacts oil accumulation in seeds

Since our analyses already established that the *aad* mutations affect the FA composition of TAGs (Supplemental Figure 7A), we finally wanted to test whether the SADs also contribute to determine the overall amount of oil stored within seeds. As a first approach, GC analyses of total FAs were conducted on mature dry seeds of the 30 mutant genotypes producing viable seeds. The results obtained were expressed on a DW basis to overcome the influence of seed size and shape on the parameter

14

studied (Figure 9A). Twelve mutant lines exhibited significantly decreased seed oil concentrations ranging from 5 to 40% with respect to the wild type. These genotypes included all the mutant lines producing twisted seeds as well as others producing perfectly normal seeds. To better characterize these depletions in oil, seeds from two severely affected genotypes were next dissected prior to GC analyses. In good agreement with the expression patterns of the SAD-coding genes in seeds (Figure 2B), the two fractions examined, embryos on one side, endosperms with seed coats attached on the other, exhibited significant losses in total FAs in the *aad* mutants considered (Figure 9B). To finally ascertain that variations of total FA concentrations reflected faithfully modifications of TAG content, total lipids extracted from seeds of a subset of genotypes were subjected to thin-layer chromatography to separate TAGs from polar lipids prior to GC analyses (Figure 9C). This approach confirmed that TAG contents were significantly decreased in seeds of the multiple *aad* mutants, whereas the total amount of polar lipids remained unchanged.

AAD1, *AAD5*, and *FAB2* are induced by WRINKLED1

The WRI1 transcription factor plays a key role in the control of oil production in seeds by inducing the expression of many FA biosynthetic genes (Marchive et al., 2014). In order to test whether one or more SAD-coding genes are under the transcriptional control of WRI1, we used a quantitative RT-PCR approach and investigated the impact of alterations in *WRI1* expression on the accumulation of the *AAD* transcripts. *AAD1*, *AAD5*, and *FAB2* appeared to be significantly downregulated in *wri1* mutant seeds compared with their wild-type counterparts (Figure 10A). In addition, transgenic *Pro35Sdual:WRI1* lines over-expressed these *AAD* genes in their vegetative parts (Figure 10B). Taken together, these data suggested that *AAD1*, *AAD5*, and *FAB2* are positive targets of WRI1. If *AAD6* transcripts appeared to be slightly over-accumulated in *Pro35Sdual:WRI1* lines, no significant changes could be detected in *wri1* seeds, ruling out the hypothesis of a transcriptional control of *AAD6* by WRI1 in this organ. Likewise, the expression patterns of *AAD2*, *AAD3*, and *AAD4*, used as negative controls in this experiment, were incompatible with a transcriptional activation by WRI1. On the contrary, *AAD3* and *AAD4* were even slightly overexpressed in *wri1* seeds (Figure 10A) and *AAD3* was repressed in *Pro35Sdual:WRI1* lines (Figure 10B).

To further evaluate the impact of WRI1 on the pattern of *AAD1*, *AAD5*, and *FAB2* promoter activity, the GUS reporter lines previously characterized were crossed with *wri1-3* so as to introgress the reporter constructs in a *wri1-3/+* context. The progeny of these plants, homozygous for the GUS reporter construct while segregating the T-DNA causing the *wri1* mutation, was analyzed by assaying *uidA* expression patterns in series of maturing embryos originating from the same silique. Under stringent conditions, no stained individuals were observed among the population of wrinkled *wri1-3* embryos, while more than one-third of the embryos exhibiting a wild-type phenotype were stained (Figure 10C).

To test WRI1 ability to directly activate the expression of *AAD1*, *AAD5*, and *FAB2*, the corresponding reporter constructs were then used in transactivation assays in *Nicotiana benthamiana* leaves (Figure 10D). The promoter sequence of the *2-OXOGLUTARATE-DEPENDENT DIOXYGENASE (ODD)* gene cloned upstream of the *uidA* reporter gene was used as a negative control. The promoter sequence of *BIOTIN CARBOXYL CARRIER PROTEIN 2* (*BCCP2*), a direct target of WRI1 (Baud et al., 2009a), served as a positive control. Reporter constructs were infiltrated alone or in combination with a vector allowing the expression of *WRI1* or *MYB115* (negative control) in leaves of *N. benthamiana*. WRI1 was able to specifically activate reporter constructs comprising *AAD1*, *AAD5*, *FAB2*, and *BCCP2* promoter sequences, showing a strong increase in GUS activity compared with the reporters co-transfected with *MYB115* or the reporters alone.

In view of these observations, a yeast one-hybrid assay was performed so as to test the interaction of WRI1 with the promoters of its three putative *AAD* targets (Supplemental Figure 14). *WRI1* fused to the coding sequence of a transcriptional activating domain (AD) was expressed in the strains containing the *HIS3* reporter gene under the control of the promoter to be tested. A specific growth of the strains on medium lacking histidine revealed an interaction between WRI1 and the promoters of *AAD1* and *AAD5* (Figure 10E). As expected, WRI1 was also able to interact with the promoter of *BCCP2* used as a positive control in this experiment (Baud et al., 2009a). Despite the presence of putative AW boxes in the *FAB2* promoter tested (Supplemental Figure 14), no interaction with WRI1 could be detected by this approach. We noted that the distance separating the putative AW boxes from the translational start was more important in the *FAB2* promoter (755 and 767 bp) than in the *AAD1* and *AAD5* promoters (71 and 74 bp, respectively). We

speculated that a different promoter topology in *FAB2* may constitute a less favorable environment for the activity of the WRI1:AD chimeric protein in yeast. For this reason, we further investigated the binding of WRI1 to the *FAB2* promoter sequence by *in vitro* electrophoretic mobility shift assay (EMSA). A recombinant WRI1 DNA-binding domain was produced, and EMSAs were performed using a DNA fragment corresponding to the region from -800 to -721 bp relative to the *FAB2* translational start codon as a probe (Figure 10F). Addition of WRI1 to the DNA fragment resulted in the formation of a shifted band (lane 3), indicating that the protein binds to the *FAB2* promoter. The binding was specific since the addition of recombinant LEC2 protein did not yield gel retardation (lane 1; negative control). What is more, competition experiments showed that increasing amounts of unlabeled nucleotides efficiently competed for WRI1 binding to the labeled probe (lanes 4–6). Taken together, these data established that *FAB2*, *AAD1*, and *AAD5* are direct targets of WRI1.

DISCUSSION

Twenty years ago, the identification of a first SAD-coding sequence in *Arabidopsis* (Kachroo et al., 2001) almost coincided with the release of the complete genome sequence of the model plant (Arabidopsis Genome Initiative, 2000). It soon appeared that *SSI2/FAB2* was part of larger family comprising seven related genes coding for AADs (Kachroo et al., 2007). Four of these isoforms, FAB2, AAD1, AAD5, and AAD6 are Δ9 SADs that produce oleic acid (Kachroo et al., 2007; Cao et al., 2010; Klinkenberg et al., 2014; this study). Since then, their functions during plant vegetative development and defense signaling have been elucidated largely through the characterization of mutants. The *fab2* mutant is an extreme dwarf as a direct result of increased stearate levels in membrane lipids (Lightner et al., 1997). Leaves of *fab2* mutant plants also exhibit hypersensitive response (HR)-like cell death lesions, accumulate high levels of salicylic acid, and constitutively overexpress pathogenesis-related genes that enhance their resistance to bacterial and oomycete pathogens for example (Kachroo et al., 2001; Kachroo et al., 2003; Kachroo et al., 2005; Gao et al., 2011). These phenotypes result from decreased oleic acid contents in cell membranes of the mutant. The *AAD6* gene is transcriptionally induced in

Agrobacterium tumafaciens-derived crown galls as a consequence of drought and hypoxia stress experienced in plant tumors (Klinkenberg et al., 2014). In these tissues, AAD6, together with other enzymes of lipid metabolism, contributes to shape the pool of unsaturated FAs.

Oleic acid and its elongated or polyunsaturated derivatives are highly accumulated in developing seeds of *Arabidopsis* (Baud et al., 2002). These acyl chains are massively produced in different tissues of the seed, where they serve for the elaboration of various acyl lipids like TAGs, polar lipids, or surface lipid polyesters (Figure 1; Figure 11). As a whole, these acyl chains account for roughly 30% of mature seed dry weight. Despite the intense desaturation of acyl chains taking place in developing seeds, simple *aad* mutants display only minor FA compositional changes (Lightner et al., 1997; Jin et al., 2017), if any, so that the identity of the SADs responsible for the production of ω-9 MUFAs in seeds has long remained elusive. Here, we demonstrate that FAB2, AAD1, AAD5, and AAD6 all participate in oleic acid production in seeds. This functional redundancy, which for a long time hampered approaches of reverse genetics, is only partial though. Altogether, the approaches implemented in this study establish that the four desaturases play critical roles at different stages of embryo development and seed maturation, and that their respective functions and importance correlate well with their transcript levels, highlighting the importance of the transcriptional activation of *AAD* genes.

FAB2, AAD1, and AAD5 are transcriptionally induced by WRI1 in *Arabidopsis* seeds

Detailed characterization of the expression patterns of SAD-coding genes based on complementary approaches like RT-qPCR and the use of the GUS reporter demonstrate the induction of these four genes during seed development. Their respective activation levels are contrasted though, with *FAB2* exhibiting the highest expression levels in all tissues of the seed. The results obtained are consistent with transcriptomic analyses of seeds and seed tissues microdissected by laser capture (Schmid and al, 2005; Belmonte et al., 2013). Altogether, these data emphasize the good correlation existing between expression of the *AADs* and the seed phenotypes observed during the characterization of the collection of corresponding mutants. In early developing embryos, only *FAB2* and *AAD5* are expressed (Supplemental Figure 15A) (Le et al., 2010; Hofman et al., 2019), which explains the embryo lethal

phenotype of *aad5 fab2* double mutants. Later during embryo elongation, *FAB2*, *AAD5*, and *AAD1* appear to be expressed in embryo epidermis (Supplemental Figure 15B) (Sakai et al., 2018). This is in good agreement with the participation of these three genes in the elaboration of the embryonic cuticle essential to prevent the adherence of the primary zygote with surrounding tissues. Finally, expression of the four *AADs* in zygotic tissues during maturation correlates well with their involvement in TAG production.

The bell-shaped expression patterns of *AAD1*, *AAD5*, and *FAB2* in seeds (Figure 2A) are similar to the profiles of several genes involved in late glycolysis and FA biosynthesis (Baud et al., 2007a; 2009a; 2010). Just like them, the three SAD-coding genes appear to be transcriptionally activated by WRI1. Consistent with this are the presence of AW *cis*-regulatory elements in their promoter sequences and the demonstrated ability of WRI1 to interact with these promoters. However, the number, sequence, and location of these AW elements within the *AAD* promoters diverge, and these differences probably account, in part, for variations in the induction levels of the three genes in seeds. In the promoters of *AAD1* and *AAD5*, single AW elements can be found close to the translational start whereas a pair of AW boxes separated by 11 base pairs is observed in a further upstream region of the *FAB2* promoter, at positions -755 and -767 from the translational start codon, respectively. This greater distance separating the putative WRI1-binding sites from the translational start codon may account for the absence of transcriptional activation of the *ProFAB2:HIS* reporter construct in yeast. Similar limitations on bait size in yeast one-hybrid assays have already been reported (Reece-Hoyce and Walhout, 2012). This suggests that the distance over which WRI1 can activate expression of target genes in the native system is higher to the one over which the WRI1-AD fusion protein can activate reporter expression in yeast. On the other hand, the presence of two AW elements in *ProFAB2* may yield better transcriptional activation *in planta*. Further analyses will now be necessary to study the affinity of WRI1 for these different AW boxes to fully elucidate the molecular mechanisms ruling the activation of FA biosynthetic genes in seeds.

The moderate induction of *AAD6* measured in seeds is unlikely to be triggered by WRI1 considering the lack of AW *cis*-regulatory element in the promoter sequence of this gene and the absence of impact of the *wri1* mutation on the accumulation of *AAD6* transcripts. Other transcriptional regulators may activate *AAD6* in seeds.

19

Considering that *AAD6* is transcriptionally induced by hypoxic conditions accompanying crown gall tumor development in roots (Klinkenberg et al., 2013), it would be interesting to study whether the low-oxygen conditions prevailing inside developing oilseeds (Porterfield et al., 1999; Vigeolas et al., 2003) may be responsible for the activation of this gene via similar regulatory mechanisms.

FAB2 and AAD5 have complementary functions essential for early embryo development

In this study, the failure to obtain *aad5 fab2* double homozygous mutants led to the unexpected discovery that the double mutant results in early developmental arrest. The first asymmetric division of the zygote, which forms two cells of different sizes, does not seem to be affected. The smaller apical cell is the founder of the embryo proper. The abortion of *aad5 fab2* embryos is associated with a cessation of division in the embryo proper at the very first stages of development. The larger basal cell normally develops into a stalk-like structure called the suspensor. Whereas the first division of the basal cell is not affected in the *aad5 fab2* mutant, further development of the suspensor seems compromised and fully formed suspensors that usually comprise six to eight cells are never observed.

An estimated 500-1.000 *EMBRYO-DEFECTIVE* (*EMB*) genes, many of them expressed throughout the plant life cycle, are essential for proper embryo development as inferred from the lethality of their mutations (Candela et al., 2011; Meinke, 2019). If many protein functions required for embryo development have been initially missed in genetic screening procedures because multiple genes encode them, at least 83 examples of double mutant combinations that produce defective embryos have been documented since then (Meinke, 2019). The *EMB* genes perform a variety of essential cellular functions. Among *emb* mutants exhibiting an early embryo arrest, proteins participating in metabolism are relatively common. Examples of *EMB* genes encoding plastidic enzymes of late glycolysis and FA synthesis include *EMB3003*, coding for a dihydrolipoamide acetyltransferase, E2 component of the pyruvate dehydrogenase complex (Lin et al., 2003), *PYRUVATE DEHYDROGENASE E1 ALPHA* (*PDH-E1 ALPHA*), E1a component of the same complex (Savage et al., 2013), *HCS1*, encoding an holocarboxylase synthetase catalyzing the addition of biotin to acetyl-CoA carboxylase (Meinke, 2019), *EMB3147*, encoding a malonyl-CoA: ACP malonyltransferase (Jung et al., 2019), *BETA-*

KETOACYL-ACP SYNTHETASE2 (*KASII/FAB1*) (Pidkowich et al., 2007), encoding a component of the FA synthase complex, and *LIP1*, encoding a lipoyl synthase (Ewald et al., 2013). *KASI* deficiency was also reported to result in disrupted embryo development before the globular stage, and it is tempting to speculate that the incomplete penetrance of this phenotype in the T-DNA mutant line characterized is the consequence of the location of the T-DNA insertion in the 5'-UTR of the gene (Wu et al., 2010). Finally, the combined deletion of the two genes encoding the octanoyltransferases LIP2P1 and LIP2P1 is embryo-lethal too (Ewald et al., 2013).

Even though terminal embryo phenotypes associated with these mutations were not all characterized with the same precision, these observations emphasize the critical role played by *de novo* FA synthesis in the embryo, probably from the first cell divisions. This FA auxotrophy provides supporting evidence that lipids cannot be transferred from the maternal tissues to the zygote, contrarily to soluble carbon sources. If not completely abolished, FA synthesis might be severely compromised in *aad5 fab2* embryos as in the mutants affected in upstream enzymatic steps of the FA biosynthesis pathway. But embryo lethality may also arise from a strong imbalance in the FA composition of its membranes, which are most certainly deprived of unsaturated acyl chains and therefore profoundly affected in their physicochemical characteristics. To this respect, it is interesting to note that in seeds of viable triple and quadruple mutants exhibiting drastic perturbations of their FA profiles, the increase in the ratio of saturated to unsaturated FAs is more pronounced in TAGs than in polar lipids (Supplemental figure 7). What is more, the slightly decreased proportion of unsaturated FAs measured in polar lipids coincides with a relative enrichment of PUFAs within the pool of unsaturated chains. In particular, the relative proportion of C18:3 almost doubles. These observations are suggestive of compensatory mechanisms meant to preserve, to a certain extent, the properties of cell membranes (e.g. fluidity, permeability) and associated biological functions in *aad* mutant backgrounds. From the decreased calcofluor staining observed at the periphery of *aad5 fab2* embryo cells, it is tempting to speculate that biosynthesis and deposition of cell wall material is one the biological functions jeopardized in mutant cells severely deprived in unsaturated FAs.

FAB2, AAD5, and AAD1 have complementary functions essential for embryo cuticle formation and embryo elongation

Cuticle is primarily known as a continuous lipophilic layer coating the periclinal cell walls of epidermal cells in aerial organs. It is composed of a FA derived polymer, known as cutin, impregnated and covered by cuticular waxes (Delude et al., 2016). In these organs, cuticle prevents non-stomatal water loss, provides mechanical strength, and protects the plant in response to biotic and abiotic stresses. What is more, juxtaposed cuticles prevent post-genital fusion of epidermal surfaces from adjacent tissues or organs, as in developing buds (Yephremov et al., 1999; Ingram and Nawrath, 2017). The embryonic cuticle also plays a key role in preventing adherence between the embryo and surrounding seed tissues, and subsequent abnormal embryo expansion and bending (Tanaka et al., 2001; Szczuka and Szczuka, 2003; Creff et al. 2019). Embryo cuticle formation involves *de novo* deposition of cuticular material at the surface of epidermal cells. Electron-dense cutin-like material is already detected at the late globular stage. However, the integrity and subsequent impermeability of this cuticle to water-soluble molecules like toluidine blue is only acquired at the torpedo stage after complete coalescence of the patches of cuticle initially deposited (Creff et al., 2019). Cuticle reinforcement then continues throughout later stages of embryogenesis. The cutin of *Arabidopsis* cotyledons taken from germinating seedlings comprises C16 and C18 dicarboxylic and ω-hydroxy FAs, plus saturated FAs ranging from C16 to C26. FAB2, AAD5, and AAD1 contribute to the production of unsaturated dicarboxylic FAs. Interestingly, in cutin as in the pool of polar lipids analyzed in seeds of *aad* mutants, levels of monounsaturated chains are significantly reduced whereas that of diunsaturated remains rather unchanged.

Intriguingly, the embryonic cuticle of *gpat4 gpat8* mutants affected in two glycerol-3-phosphate acyltransferases involved in cutin biosynthesis (Li et al., 2007) remains partially functional and no twisted seeds are observed in this genetic background despite a strong reduction in cutin monomers measured on cotyledons of germinated seedlings (Creff et al., 2019). Conversely, the embryos of some *aad* double mutants characterized in this study display a twisted phenotype associated with a dysfunctional cuticle when the total cutin load of their cotyledons remains unchanged. This apparent paradox suggests that the monomer composition of cutin may prevail over the total amount of material deposited with respect to cuticle functionality. The *gpat4 gpat8* mutants and *aad* double mutants indeed display contrasted compositional changes: in the former, a tremendous decrease in all dicarboxylic and

ω-hydroxy FAs is observed while contents of saturated FAs remain unchanged, whereas the latter display a specific decrease in C18:1 dicarboxylic FA accompanied by an enrichment in saturated chains. Unfortunately, our knowledge about the precise structure of surface lipid polyesters is limited, preventing us from further speculating about a precise biological function of any of its components in the context of embryo development. Then, the hypothesis of an impact of the *aad* mutations on other components of the cuticle cannot be entirely ruled out. As previously mentioned, the cuticle observed in aerial parts of the plant associates cutin with waxes, made of a mixture of very-long chain aliphatic compounds. Given the difficulty to harvest embryonic tissues and the usual low abundance of cuticular waxes, we ignore whether such compounds are also present at the surface of embryo cells and how their synthesis and deposition is affected in the mutants studied. As for the embryo sheath made of endosperm-derived material rich in glycoproteins and deposited outside the embryonic cuticle during embryogenesis (Moussu et al., 2017), nothing is known about its interactions with the underlying cuticle, if any. Considering the essential lubrication function of this sheath that also facilitates the movement of the embryo relative to the degenerating endosperm, it would be interesting to further characterize its formation and behavior in mutant backgrounds affected in cuticle biosynthesis to learn more about the putative interplay between these two protective layers that coat the embryo.

Four SADs redundantly contribute to storage lipid production in zygotic tissues

The fine characterization of the seed oil content of the *aad* mutants described in this study finally establishes the redundant contribution of the four AADs in storage lipid production in the two zygotic tissues of the seed. The *aad* mutations tremendously affect the FA composition of storage lipids. In the quadruple *aad* mutants, the proportion of C18:0 in seed oil is more than seven times higher than that of the wild type, exceeding 25 Mol % while total levels of saturated FAs approach 50 Mol %. Oils with such elevated levels of C18:0 are oxidatively stable whilst displaying relatively high melting temperature. They are useful for solid fat applications, both for their cooking properties and health benefits (Clemente and Cahoon, 2009; Ruddle et al., 2013). Since the vegetable oils naturally rich in C18:0 are scarce, a number of genetic approaches have been pursued to develop elevated stearic germplasm lines,

mostly in soybean (*Glycine max*) and in Brassica species. Mutations targeting SAD-coding genes were used with varying degrees of success as a mean to elevate C18:0 (Ruddle et al., 2013; Lakhssassi et al., 2017).

Unfortunately, high stearate lines often display deleterious characteristics like poor germination, reduced growth or low seed yield that preclude their commercial exploitation. It is interesting to note that the enrichment of seed oil in C18:0 in several of the mutant lines presented in this study (e.g. the quadruple mutants) can be dissociated from some of the most deleterious phenotypes caused by certain *aad* mutations. First, embryos of the quadruple mutants are not twisted, a phenotype usually associated with delayed or prevented cotyledon emergence during germination that can impair autotrophy establishment (Doll et al., 2020). Second, the quadruple mutants studied carry the leaky *fab2-1* mutation affecting the induction of *FAB2* in seeds without compromising the expression of the desaturase-coding gene in vegetative organs, so that they are not dwarf. Unfortunately, it seems more difficult to fully dissociate increased stearate levels from reduced seed oil contents, even though the two traits are not strictly correlated in the collection of mutants characterized. Not surprisingly, SAD activity appears as one important determinant of oil concentration in *Arabidopsis* seeds. Despite the existence of an alternative pathway able to channel saturated acyl chains into the acyl-CoA pool, the overall flux of carbon into TAGs is decreased in mutants combining several *aad* mutations, illustrating the limited plasticity of the oil biosynthetic network.

In conclusion, if the partial functional redundancy of the four SADs expressed in seeds of *Arabidopsis* has long delayed the elucidation of their biological functions in this complex organ, the long-term approach consisting in combining knockout or leaky mutations for each of the corresponding genes has provided us with a unique opportunity to assess the importance of SAD activity all along seed development. From the first cell divisions taking place in the embryo until the phase of storage compound accumulation, the SADs synthesize unsaturated FAs used for the elaboration of different classes of lipids that play several critical roles in seed development.

METHODS

Plant material and growth conditions

T-DNA mutant lines (*aad1-1*, N666506; *aad1-3*, N858166; *aad5-1*, N661145; *aad5-2*, N657908; *aad5-3*, N451517; *aad6-1*, N618643; *fab2-1*, N828229; *fab2-2* N536854; *fab2-3*, N872133) were ordered from the NASC (http://arabidopsis.info). The *fab2-2/ssi2* allele was previously described in Bryant *et al.* (2016), whereas *aad5-1* and *aad5-2* were described in Jin *et al.* (2017). Plants were cultured as described in Baud et al. (2007a). To sample embryo and endosperm fractions, seeds excised from siliques were dissected using a scalpel and dissecting tweezers under an optical glass binocular magnifier. Material used for RNA extraction was frozen in liquid nitrogen immediately after harvest, and then stored at -80°C.

Molecular characterization of T-DNA mutants

Plant genomic DNA flanking the T-DNA borders of the mutants were amplified by PCR (Supplemental Table 1) and sequenced to confirm the flanking sequence tags identified. Homozygous lines were then isolated for further characterization. RT-PCR analyses were ultimately performed to analyze gene expression in mutant backgrounds (Supplemental Table 2).

Constructs and plant transformation

The sequences of primers used for DNA amplification are indicated in Supplemental Table 3.

For construction of the *ProAAD1:uidA*, *ProAAD4:uidA*, *ProAAD4:AAD4g:uidA*, *ProAAD5:uidA*, *ProAAD5:AAD5g:uidA*, *ProAAD6:uidA*, *ProFAB2:uidA*, and *ProFAB2:FAB2g:uidA* transgenes, DNA fragments comprising either promoter sequences alone or promoter sequences plus open reading frames were amplified with the proofreading Pfu Ultra DNA polymerase (Stratagene) from Col-0 genomic DNA. The PCR products were introduced by BP recombination into the pDONR207 entry vector (Invitrogen) and transferred into the destination vector pGWB3 (Nakagawa et al., 2007) by LR recombination. The resulting binary vector was electroporated into *Agrobacterium tumefaciens* C58C[1] strain and used for agroinfiltration of flower buds of *Arabidopsis* (Bechtold et al., 1993). Primary transformants were selected on MS medium containing hygromycin (50 mg.l^{-1}) and transferred to soil for further characterization. For each construct, between 14 and 22 independent transgenic lines were analyzed. Construction of the *ProAAD2:uidA* and

ProAAD3:uidA transgenes was previously described in Troncoso-Ponce et al. (2016a).

For construction of the *ProAAD5:AAD5g* and *ProFAB2:FAB2g* transgenes, DNA fragments encompassing *AAD5* or *FAB2* were amplified with the proofreading Pfu Ultra DNA polymerase (Stratagene) from Col-0 genomic DNA. The PCR products were introduced by BP recombination into the pDONR207 entry vector (Invitrogen) and transferred into the destination vector pBIB-Hyg-GTW (Dubos et al., 2008) by LR recombination. Primary transformants were selected on MS medium containing hygromycin (50 mg.l^{-1}).

For construction of the *ProFAB2:AADc* transgenes, a pProFAB2-R1R2-Hygro vector was first prepared as follows: region -1,000 to -1 bp relative to the *FAB2* translational start codon was amplified with the proofreading Pfu Ultra DNA polymerase (Stratagene) from Col-0 genomic DNA and the PCR product was digested with *Hin*dIII and *Asc*I to be cloned into the pMDC32 vector (Curtis and Grossniklaus, 2003) digested with *Hin*dIII and *Asc*I, thus replacing the 2X35S cassette. The *AAD* cDNAs were then cloned into the pDONR207 entry vector (Invitrogen) as described in Troncoso-Ponce et al. (2016a) and ultimately transferred into the destination vector pProFAB2-R1R2-Hygro by LR recombination. Primary transformants were selected on MS medium containing hygromycin (50 mg.l^{-1}).

Yeast one-hybrid experiments

For construction of the *ProAAD1:HIS*, *ProAAD5:HIS* and *ProFAB2:HIS* transgenes, regions -1,000 to -1 bp relative to the translational start codon of the *AAD* genes were amplified with the proofreading Pfu Ultra DNA polymerase (Stratagene) from Col-0 genomic DNA and the PCR products were cloned into the pHISi vector (Clontech) using the ligation-independent cloning system (LIC) described in Kelemen et al. (2016). The pHISi reporter plasmid containing a 180-bp fragment of the *BCCP2* promoter was constructed as previously described (Baud et al., 2009a). The pHISi reporter plasmids were integrated into the yeast strain YM4271 (Liu et al., 1993). Cloning of the *WRI1* cDNA in pDEST22 was described in To et al. (2012). YM4271 yeast cells presenting the *HIS3* reporter gene under the control of plant promoters (see above) were transformed with pDEST22 according to the AcLi/SSDNA/PEG method (Gietz and Woods, 2002). Transformants were selected on appropriate medium.

Electrophoretic mobility-shift assays

Construction of the expression plasmid by insertion of a truncated version of *WRI1* cDNA encoding the WRI DNA-binding domain (DBD; amino acids 52-237) in the pET_trx1a vector was previously described in Baud et al. (2009a). The WRI1 DBD was expressed using *Escherichia coli* strain RosettaBlue(DE3)pLysS (Novagen). After induction by 0.5 mM isopropyl-ß-D-thiogalactopyranoside in Luria-Bertani buffer, cells were grown overnight at 17°C. Cell lysis and protein purification were described in Baud et al. (2009a). Recombinant LEC2 proteins used as negative controls were obtained as described in Baud et al. (2009b).

To prepare DNA probes, complementary biotin-labeled (at the 5' end) oligonucleotides (Eurofins MWG Operon) were annealed. For DNA-binding assays, 400 µg of recombinant proteins were incubated with 20 fmol probe in binding buffer (20 mM Tris HCl pH 8, 250 mM NaCl, 2 mM MgCl$_2$, 1% glycerol, 1 mg.ml^{-1} BSA, 1 mM DTT). For competition assays, the unbiotinylated competitor was incubated briefly with the recombinant protein before the biotinylated probe was added. After addition of the biotinylated probe, reactions were incubated 30 min at room temperature, then fractionated at 4°C by 6% PAGE. Electrophoretic transfer to nylon membrane and detection of the biotin-labeled DNA were carried out according to the manufacturer's instructions (Chemiluminescent Nucleic Acid Detection Module, PIERCE) using an ImageQuant LAS 4000 system (GE Healthcare).

RNA analyses

RNA extraction, reverse transcription, RT-PCR, and real-time RT quantitative PCR were performed as previously described (Baud et al., 2004). The sequences of primers used for RT-PCR and real-time RT-qPCR are indicated in Supplemental Tables 2 and 4. Purity of the different seed fractions sampled was assessed as described in Barthole et al. (2014). Briefly, marker genes for each of the fractions sampled, namely *ZHOUPI* (*ZOU*; endosperm-specific) and *At2g23230* (embryo-specific) were quantified on cDNAs prepared from these fractions, thus confirming that no significant contamination occurred between fractions.

Lipid analyses

Total fatty acid analyses were performed as previously described (Li et al., 2006) on pools of *Arabidopsis* seeds or seed fractions.

To analyze lipid polyester composition in cotyledons, batches of 100 cotyledons were collected and immersed in hot isopropanol for 10 min at 80°C. For seed coat analyses, 50 mg of dry seeds were ground in isopropanol, and then heated for 30 min at 85°C. After cooling, samples were extensively delipidated to extract the soluble lipids, dried, and then depolymerized as previously described (Domergue et al., 2010). Extraction, derivatization, and analysis by GC-MS were performed as previously described (Domergue et al., 2010).

To analyze polar lipids and triacylglycerols, batches of 50 seeds were ground in 2.4 ml of precooled chloroform/methanol/formic acid/water (10:10:1:1, v/v/v/v) and incubated at -20°C overnight. The mixture was centrifuged at 7,500 g for 10 min at 4°C to pellet the cell debris. Lipids of the pellet were reextracted in 0.88 ml of precooled chloroform/methanol/water (5:5:1, v/v/v). Then, 1.2 ml of cooled Hajra solution (KCl 2 M and H_3PO_4 0.2 M) was added to the pooled supernatants. After shaking and centrifugation (7,500 g for 10 min at 4°C), the lower phase containing lipids was collected and evaporated with a stream of N_2. Lipids were finally resuspended in chloroform. Separation on thin-layer chromatography plates and subsequent analysis of lipid spots by gas chromatography was previously described in Baud *et al*. (2002).

Microscopy

Histochemical detection of GUS activity and bright-field microscope observations were carried out as described in Baud et al. (2007a). Mature pollen viability was studied as described by Alexander (1969). Toluidine blue staining of seedlings was previously described in Xing et al. (2013). To obtain scanning electron micrographs, seeds were mounted onto a Peltier cooling stage using adhesive discs (Deben) and observed with a SH-1500 tabletop scanning electron microscope (Hirox).

To observe longitudinal sections of developing embryos, seeds were dissected and fixed as described in Belcram et al. (2016). After fixation and rehydration, samples were cleared for 2 h in a freshly prepared 0.2 N NaOH, 1% SDS solution, rinsed 10 min in distilled water, and incubated for 5 weeks in SCALE solution (0.1% Triton X-100, 10% glycerol, 25% urea). Samples were then washed for 5 min in distilled water and immersed for 30 min in a staining solution containing Fluorescent

Brightener 28 (0.25%). They were finally mounted in mounting medium (Citifluor). Fluorescence was recorded after a 405 nm diode laser excitation and a selective emission of 415-448 nm. Acquisitions were made with an inverted Zeiss Observer Z1 spectral confocal laser microscope LSM 710 using a Plan-Apochromat 40x/1.3 oil DIC M27 objective. Pictures showing mid-plane longitudinal sections of embryos were captured.

Auramine O staining was realized as previously described (Fiume et al., 2016). Acquisitions were made with an inverted Zeiss Observer Z1 spectral confocal laser microscope LSM 710 using a C-Apochromat 63x/1.2 water objective and a 488 nm argon laser line. Fluorescence emission was detected between 494 and 546 nm for Auramine O, 679 and 759 nm for chlorophyll.

Accession Numbers

Sequence data from this article can be found in the EMBL/GenBank data libraries under accession numbers: *BCCP2*, At5g15530; *AAD1,* At5g16240; *AAD2,* At3g02610; *AAD3,* At5g16230; *AAD4,* At3g02620; *AAD5,* At3g02630; *AAD6*, At1g43800; *EF1αA4*, At5g60390; *EMB3003*, At1g34430; *EMB3147*, At2g30200; *FAB2/SSI2*, At2g43710; *HCS1*, At2g25710; *KASII/FAB1*, At1g74960; *LIP1*, At5g08415; *LIP1P1*, At4g31050; *LIP2P2*, At1g47578; *PDH-E1 ALPHA*, At1g01090; *LEC2*, At1g28300; *WRI1*, At3g54320; and *ZOU/RGE1*, At1g49770.

Supplemental Data

Supplemental Figure 1. Complementary information for the characterization of the patterns of mRNA accumulation among the *AAD* family.

Supplemental Figure 2. Complementary information for the pattern of activity of GUS reporter constructs.

Supplemental Figure 3. Complementary information for the sequences of *Arabidopsis* AADs.

Supplemental Figure 4. Complementary information for the characterization of *fab2* mutants expressing *ProFAB2:AADc* constructs.

Supplemental Figure 5. Phenotype of *aad5/+ fab2* mutants.

Supplemental Figure 6. Complementary information for the biochemical characterization of seed fractions from a subset of *aad* mutants.

AUTHORS CONTRIBUTIONS

A.T., D.D.V., D.V., F.D., K.B., and H.E. performed the research and analyzed the data, L.L. designed the research, G.B., S.B., and S.K. designed and performed the research, analyzed the data, and wrote the article.

REFERENCES

Alexander, M.P. (1969). Differential staining of aborted and nonaborted pollen. Stain Technol. 44: 117-122.

Arabidopsis Genome Initiative (2000). Analysis of the genome sequence of the flowering plant *Arabidopsis thaliana*. Nature 14: 796-815.

Arnold, K., Bordoli, L., Kopp, J., and Schwede, T. (2006). The SWISS-MODEL workspace: a web-based environment for protein structure homology modelling. Bioinformatics 22: 195-201.

Barthole, G., To, A., Marchive, C., Brunaud, V., Soubigou-Taconnat, L., Berger, N., Dubreucq, B., Lepiniec, L., and Baud, S. (2014). MYB118 represses endosperm maturation in seeds of *Arabidopsis*. Plant Cell 26: 3519-3537.

Bates P.D., Stymne S., and Ohlrogge J. (2013). Biochemical pathways in seed oil synthesis. Curr. Opin. Plant Biol. 16: 1-7.

Baud, S., Boutin, J.P., Miquel, M., Lepiniec, L., and Rochat, C. (2002). An integrated overview of seed development in *Arabidopsis thaliana* ecotype WS. Plant Physiol. Biochem. 40: 151-160.

Baud, S., Vaultier, M.-N., and Rochat, C. (2004). Structure and expression profile of the sucrose synthase multigene family in Arabidopsis. J. Exp. Bot. 55: 397-409.

Baud, S., Wuillème, S., Dubreucq, B., de Almeida, A., Vuagnat, C., Lepiniec, L., Miquel, M., and Rochat, C. (2007a). Function of plastidial pyruvate kinase in seeds of *Arabidopsis thaliana*. Plant J. 52: 405-419.

Baud, S., Santos Mendoza, M., To, A., Harscoët, E., Lepiniec, L., and Dubreucq, B. (2007b). WRINKLED1 specifies the regulatory action of LEAFY COTYLEDON2 towards fatty acid metabolism during seed maturation in Arabidopsis. Plant J. 50: 825-838.

Baud, S., Dubreucq, B., Miquel, M., Rochat, C., and lepiniec, L. (2008) Storage reserve accumulation in Arabidopsis: Metabolic and developmental control of seed filling. The Arabidopsis Book 6: 1-24.

Baud, S., Wuillème, S., To, A., Rochat, C., and Lepiniec, L. (2009a). Role of WRINKLED1 in the transcriptional regulation of glycolytic and fatty acid biosynthetic genes in Arabidopsis. Plant J. 60: 933-947.

Baud, S., Reinhard Dichow, N., Kelemen, Z., d'Andréa, S., To, A., Berger, N., Canonge, M., Kronenberger, J., Viterbo, D., Dubreucq, B., Lepiniec, L., Chardot, T., and Miquel, M. (2009b) Regulation of HSD1 in seeds of *Arabidopsis thaliana*. Plant Cell Physiol. 50: 1463-1478.

Baud, S., and Lepiniec, L. (2010). Physiological and developmental regulation of seed oil production. Prog. Lipid Res. 49: 235-249.

Baud, S., Feria Bourrellier, A.B., Azzopardi, M., Berger, A., Dechorgnat, J., Daniel-Vedele, F., Lepiniec, L., Miquel, M., Rochat, C., Hodges, M., and Ferrario-Méry, S. (2010). PII is induced by WRINKLED1 and fine-tunes fatty acid composition in seeds of *Arabidopsis thaliana*. Plant J. 64: 291-303.

Bechtold, N., Ellis, J., and Pelletier, G. (1993). *In planta* infiltration of adult Arabidopsis plants. C. R. Acad. Sci. Paris Life Sci. 316: 1194-1199.

Beeckman, T., De Rycke, R., Viane, R., and Inze, D. (2000). Histological study of

seed coat development in *Arabidopsis thaliana*. J. Plant Res. 113: 139-148.

Belcram, K., Palauqui, J.-C., and Pastuglia, M. (2016). Studying cell division plane positioning in early-stage embryos. Methods Mol. Biol. 1370: 183-195.

Belmonte, M.F., Kirkbride, R.C., Stone, S.L., Pelletier, J.M., Bui, A.Q., Yeung, E.C., Hashimoto, M., Fei, J., Harada, C.M., Munoz, M.D., Le, B.H., Drews, G.N., Brady, S.M., Goldberg, R.B., and Harada, J.J. (2013). Comprehensive developmental profiles of gene activity in regions and subregions of the Arabidopsis seed. Proc. Natl Acad. Sci. USA 110: 435-444.

Bewley, J.D. (1997). Seed germination and dormancy. Plant Cell 9: 1055-1066.

Bordoli, L., Kiefer, F., Arnold, K., Benkert, P., Battey, J., and Schwede, T. (2009). Protein structure homology modelling using SWISS-MODEL workspace. Nat. Protoc. 4: 1-13.

Bryant, F.M., Munoz-Azcarate, O., Kelly, A.A., Beaudoin, F., Kurup, S., and Eastmond, P.J. (2016). ACYL-ACYL CARRIER PROTEIN DESATURASE2 and 3 are responsible for making omega-7 fatty acids in the Arabidopsis aleurone. Plant Physiol. 172: 154-162.

Buda, G.J., Isaacson, T., Matas, A.J., Paolillo, D.J., and Rose, J.K. (2009). Three-dimensional imaging of plant cuticle architecture using confocal scanning laser microscopy. Plant J. 60:378-385.

Cahoon, E.B., Shah, S., Shanklin, J., and Browse, J. (1998). A determinant of substrate specificity predicted from the acyl-acyl carrier protein desaturase of developing cat's claw seed. Plant Physiol. 117: 593-598.

Candela, H., Pérez-Pérez, J.M., and Micol J.L. (2011). Uncovering the post-embryonic functions of gametophytic- and embryonic-lethal genes. Trends Plant Sci. 16: 336-345.

Cao, Y., Xian, M., Yang, J., Xu, X., Liu, W., and Li, L. (2010). Heterologous expression of stearoyl-acyl carrier protein desaturase (S-ACP-DES) from *Arabidopsis thaliana* in *Escherichia coli*. Protein Expr. Purif. 69: 209-214.

Cernac, A., and Benning, C. (2004). WRINKLED1 encodes an AP2/EREB domain protein involved in the control of storage compound biosynthesis in Arabidopsis. Plant J. 40: 575-585.

Clemente, T.E., and Cahoon, E.B. (2009). Soybean oil: genetic approaches for modification of functionality and total content. Plant Physiol. 151: 1030-1040.

Creff, A., Brocard, L., Joubès, J., Taconnat, L., Doll, N.M., Marsollier, A.-C., Pascal, S., Galleti, R., Boeuf, S., Moussu, S., Widiez, T., Domergue, F., and Ingram, G. (2019). A stress-response-related inter-compartmental pathway regulates embryonic cuticle integrity in Arabidopsis. PLoS Genet. 15: e1007847.

Curtis, M., and Grossniklaus, U. (2003). A Gateway TM cloning vector set for high-throughput functional analysis of genes in plants. Plant Physiol. 133: 462-469.

Delude, C., Moussu, S., Joubès, J., Ingram, G., and Domergue, F. (2016). Plant surface lipids and epidermis development. Subcell. Biochem. 86: 287-313.

Doll, N.M., Bovio, S., Gaiti, A., Marsollier, A.-C., Chamot, S., Moussu, S., Widiez, T., and Ingram, G. (2020). The endosperm-derived embryo sheath is an anti-adhesive structure that facilitates cotyledon emergence during germination. Curr. Biol. 30: 909-915.

Domergue, F., Vishwanath, S.J., Joubès, J., Ono, J., Lee, J.A., Bourdon, M., Alhattab, R., Lowe, C., Pascal, S., Lessire, R., and Rowland, O. (2010). Three Arabidopsis fatty acyl-coenzyme A reductases, FAR1, FAR4, and FAR5, generate primary fatty alcohols associated with suberin deposition. Plant Physiol. 153: 1539-1554.

Dubos, C., Le Gourrierec, J., Baudry, A., Huep, G., Lanet, E., Debeaujon, I., Routaboul, J.-M., Alboresi, A., Weisshaar, B., and Lepiniec, L. (2008). MYBL2 is a new regulator of flavonoid biosynthesis in *Arabidopsis thaliana*. Plant J. 55: 940-953.

Ewald, R., Hoffmann, C., Neuhaus, E., and Bauwe, H. (2013). Two redundant octanoyltransferases and one obligatory lipoyl synthase provide protein-lipoylation autonomy to plastids of Arabidopsis. Plant Biol. 16: 35-42.

Fiume, E., Guyon, V., Remoué, C., Magnani, E., Miquel, M., Grain, D., and Lepiniec, L. (2016). TWS1, a novel small protein, regulates various aspects of seed and plant development. Plant Physiol. 172: 1732-1745.

Gao, Q.-M., Venugopal, S., Navarre, D., and Kachroo, A. (2011). Low oleic acid-derived repression of jasmonic acid-inducible defense responses requires the WRKY50 and WRKY51 proteins. Plant Physiol. 155: 464-476.

Gietz, R.D., and Woods, R.A. (2002). Transformation of yeast by lithium acetate/single-stranded carrier DNA/polyethylene glycol methods. Methods Enzymol. 350: 87-96.

Harwood, J. (1996). Recent advances in the biosynthesis of plant fatty acids. Biochim. Biophys. Acta 1301: 7-56.

Hofmann, F., Schon, M.A., and Nodine, M.D. (2019).The embryonic transcriptome of *Arabidopsis thaliana*. Plant Reprod. 32:77-91.

Ingram, G., and Nawrath, C. (2017). The roles of cuticle in plant development: organ adhesions and beyond. J. Exp. Bot. 68: 5307-5321.

Jin C., Li D., Gao C., Liu K., Qi S., Duan S., Li Z., Gong J., Wang J., Hai J., and Chen M. (2017). Conserved function of ACYL-ACYL CARRIER PROTEIN DESATURASE5 on seed oil and oleic acid biosynthesis between *Arabidopsis* and *Brassica napus*. Front Plant Sci 8: 1319.

Jung, S.H., Kim, R.J., Kim, K.J., Lee, D.H., and Suh, M.C. (2019). Plastidial and mitochondrial malonyl CoA-ACP malonyltransferase is essential for cell division and its overexpression increases storage oil content. Plant Cell Physiol. 60: 1239-1249.

Kachroo, A., Lapchyk, L., Fukushige, H., Hildebrand, D., Klessig, D., and Kachroo, P. (2003). Plastidial fatty acid signaling modulates salicylic acid- and jasmonic acid-mediated defense pathways in the Arabidopsis *ssi2* mutant. Plant Cell 15: 2952-2965.

Kachroo, A., Shanklin, J., Whittle, E., Lapchyk, L., Hildebrand, D., and Kachroo, P. (2007). The Arabidopsis stearoyl-acyl carrier protein-desaturase family and the accumulation of leaf isoforms to oleic acid synthesis. Plant Mol. Biol. 63: 257-271.

Kachroo, P., Shanklin, J., Shah, J., Whittle, E.J., and Klessig, F. (2001). A fatty acid desaturase modulates the activation of defense signaling pathways in plants. Proc. Natl Acad. Sci. USA 98: 9448-9453.

Kachroo, P., Venugopal, S.C., Navarre, D.A., Lapchyk, L., and Kachroo, A. (2005). Role of salicylic acid and fatty acid desaturation pathways in *ssi2*-mediated signaling. Plant Physiol. 139: 1717-1735.

Kelemen, Z., Przybyla-Toscano, J., Tissot, N., Lepiniec, L., and Dubos, C. (2016). Fast and efficient cloning of *Cis*-regulatory sequences for high-throughput yeast one-hybrid analyses of transcription factors. Methods Mol. Biol. 1482: 139-149.

Kim M.J., Jang I.-C., and Chua N.-H. (2016). The mediator complex MED15 subunit mediates activation of downstream lipid-related genes by the WRINKLED1 transcription factor. Plant Physiol. 171:1951-1964.

Klinkenberg, J., Faist, H., Saupe S., Lambertz, S., Krischke, M., Stingl, N., Fekete, A., Mueller, M.J., Feussner, I., Hedrich, R., and Deeken, R. (2014). two fatty acid desaturases, STEAROYL-ACYL CARRIER PROTEIN Δ^9-DESATURASES6 and FATTY ACID DESATURASE3, are involved in drought and hypoxia stress signaling in Arabidopsis crown galls. Plant Physiol. 164: 570-583.

Lakhssassi, N., Colantonio, V., Flowers, N.D., Zhou, Z., Henry, J., Liu, S., and Meksem, K. (2017). Stearoyl-acyl carrier protein desaturases mutations unconver an impact of stearic acid in leaf and nodule structure. Plant Physiol. 174: 1531-1543.

Laux, T., and Jürgens, G. (1997) Embryogenesis: A new start in life. Plant Cell 9: 989-1000.

Le, B.H., Cheng, C., Bui, A.Q., Wagmaister, J.A., Henry, K., Pelletier, J., Kwong, L., Belmonte, M., Kirkbride, R., Horvath, S., Drews, G.N., Fischer, R.L., Okamuro, J.K., Harada, J.J., and Goldberg, R.B. (2010). Global analysis of gene activity during Arabidopsis seed development and identification of seed-specific transcription factors. Proc. Natl. Acad.Sci. USA 107: 8063-8070.

Lepiniec, L., Devic, M., Roscoe, T.J., Bouyer, D., Zhou, D.-X., Boulard, C., Baud, S., and Dubreucq, B. (2018) Molecular and epigenetic regulations and functions of the LAFL transcriptional regulators that control seed development. Plant Reprod. 31: 291-307.

Li, Y., Beisson, F., and Ohlrogge, J. (2006). Oil content of Arabidopsis seeds: the influence of seed anatomy, light and plant-to-plant variation. Phytochemistry 67: 904-915.

Li, Y., Beisson, F., Koo, A.J.K., Molina, I., Pollard, M., and Ohlrogge, J. (2007). Identification of acyltransferases required for cutin biosynthesis and production of cutin with suberin-like monomers. Proc. Natl Acad. Sci. USA 46: 18339-18344.

Lightner, J., Wu, J., and Browse, J. (1994). A mutant of Arabidopsis with increased levels of stearic acid. Plant Physiol. 106: 1443-1451.

Lightner, J., Lark, E., James, D., and Browse, J. (1997). Novel mutations affecting leaf stearate content and plant size in *Arabidopsis*. Theor. Appl. Genet. 94: 975-981.

Lin, M., Behal, R., and Oliver, D.J. (2003). Disruption of *plE2*, the gene coding for the E2 subunit of the plastid pyruvate dehydrogenase complex, in *Arabidopsis* causes an early embryo lethal phenotype. Plant Mol. Biol. 52: 865-872.

Liu, J., Wilson, T.E., Milbrandt, J., and Johnston, M. (1993). Identifying DNA-binding sites and analyzing DNA-binding domains using a yeast selection system. Methods 5: 125-137.

Loubéry, S., De Giorgi, J., Utz-Pugin, A., Demonsais, L., and Lopez-Molina, L. (2018). A maternally deposited endosperm cuticle contributes to the physiological defects of *transparent testa* seeds. Plant Physiol. 177: 1218-1233.

Maeo K., Tokuda T., Ayame A., Mitsui N., Kawai T., Tsukogashi H., Ishiguro S., and Nakamura K. (2009). An AP2-type transcription factor, WRINKLED1, of *Arabidopsis thaliana* binds to the AW-box sequence conserved among proximal upstream regions of genes involved in fatty acid synthesis. Plant J 60: 476-487.

Marchive C., Nikovics K., To A., Lepiniec L., and Baud S. (2014). Transcriptional regulation of fatty acid production in higher plants: Molecular bases and biotechnological outcomes. Eur. J. Lipid Sci. Technol. 116: 1332-1343.

Meinke, D.W. (2019). Genome-wide identification of *EMBRYO-DEFECTIVE* (*EMB*) genes required for growth and development in Arabidopsis. New Phytol. 226: 306-325.

Moussu S., Doll N.M., Chamot S., Brocard L., Creff A., Fourquin C., Widiez T., Nimchuk Z.L., and Ingram G. (2017). ZHOUPI and KERBEROS mediate embryo/endosperm separation by promoting the formation of an extracuticular sheath at the embryo surface. Plant Cell 29: 1642-1656.

Nakagawa, T., Kurose, T., Hino, T., Tanaka, K., Kawamukai, M., Niwa, Y., Toyooka, K., Matsuoka, K., Jinbo, T., and Kimura, T. (2007). Development of series of Gateway binary vectors, pGWBs, for realizing efficient construction of fusion genes for plant transformation. J. Biosci. Bioeng. 104: 34-41.

Penfield, S., Rylott, E.L., Gilday, A.D., Graham, S., Larson, T.R., and Graham, I.A. (2004). Reserve mobilization in the Arabidopsis endosperm fuels hypocotyl elongation in the dark, is dependent of abscisic acid, and requires *PHOSPHOENOLPYRUVATE CARBOXYKINASE1*. Plant Cell 16: 2705-2718.

Pidkowich, M.S., Nguyen, H.T., Heilmann, I., Ischebeck, T., and Shanklin, J. (2007). Modulating seed ß-ketoacyl-acyl carrier protein synthase II converts the composition of a temperate seed oil to that of a palm-like tropical oil. Proc. Natl Acad. Sci. USA 104: 4742-4747.

Porterfield, D.M., Kuang, A., Smith, P.J.S., Crispi, M., and Musgrave, M.E. (1999). Oxygen-depleted zones inside reproductive structures of Brassicaceae: implications for oxygen control of seed development. Can. J. Bot. 77: 1439-1446.

Reece-Hoyes J.S., and Walhout, A.J.M. (2012). Yeast one-hybrid assays: a historical and technical perspective. Methods 57: 441-447.

Ruddle II, P., Whetten, R., Cardinal, A., Upchurch, R.G., and Miranda, L. (2013). Effect of a novel mutation in a Δ9-stearoyl-ACP-desaturase on soybean seed oil composition. Theor. Appl. Genet. 126: 241-249.

Sakai, K., Taconnat, L., Borrega, N., Yansouni, J., Brunaud, V., Paysant-Le Roux, C., Delannoy, E., Martin Magniette, M.-L., Lepiniec, L., Faure, J.D., Balzergue, S., and Dubreucq, B. (2018) .Combining laser-assisted microdissection (LAM) and RNA-seq allows to perform a comprehensive transcriptomic analysis of epidermal cells of Arabidopsis embryo. Plant Methods 14: 10.

Savage, L.J., Imre, K.M., Hall, D.A., and Last, R.L. (2013). Analysis of essential Arabidopsis nuclear genes encoding plastid-targeted proteins. PLoS ONE 8: e73291.

Shamloul, M., Trusa, J., Mett, V., and Yusibov, V. (2014). Optimization and utilization of *Agrobacterium*-mediated transient protein production in *Nicotiana*. J. Vis. Exp. 86: 51204.

Shanklin J., and Cahoon E.B. (1998). Desaturation and related modifications of fatty acids. Annu Rev Plant Physiol Plant Mol Biol. 49: 611-641.

Schmid, M., Davison, T.S., Henz, S.R., Pape, U.J., Demar, M., Vingron, M., Scholkopf, B., Weigel, D., and Lohmann, J.U. (2005). A gene expression map of *Arabidopsis thaliana* development. Nat. Genet. 37: 501-506.

Szczuka, E., and Szczuka, A. (2003). Cuticle fluorescence during embryogenesis of *Arabidopsis thaliana* (L.) Heynh. Acta Biol. Cracov. Bot. 45: 63-67.

Tanaka, H., Onouchi, H., Kondo, M., Hara-Nishimura, I., Nishimura, M., Machida, C., and Machida, Y. (2001). A subtilisn-like serine protease is required for epidermal surface formation in Arabidopsis embryos and juvenile plants. Development 128: 4681-4689.

Tanaka, T., Tanaka, H., Machida, C., Watanabe, M., and Machida, Y. (2004). A new method for rapid visualization of defects in leaf cuticle reveals five intrinsic patterns of surface defects in *Arabidopsis*. Plant J. 37: 139-146.

To, A., Joubès, J., Barthole, G., Lécureuil, A., Scagnelli, A., Jasinski, S., Lepiniec, L., and Baud S. (2012). WRINKLED transcription factors orchestrate tissue-specific regulation of fatty acid biosynthesis in *Arabidopsis*. Plant Cell 24: 5007-5023.

Troncoso-Ponce, M.A., Barthole, G., Tremblais, G., To, A., Miquel, M., Lepiniec, L., and Baud, S. (2016a). Transcriptional activation of two delta-9 palmitoyl-ACP desaturase genes by MYB115 and MYB118 is critical for biosynthesis of omega-7 monounsaturated fatty acids in the endosperm of Arabidopsis seeds. Plant Cell 28: 2666-2682.

Troncoso-Ponce, M.A., Nikovics K., Marchive C., Lepiniec L., and Baud S. (2016b). New insights on the organization and regulation of the fatty acid biosynthetic network in the model higher plant *Arabidopsis thaliana*. Biochimie 120: 3-8.

Tsuwamoto, R., Fukuoka, H., and Takahata, Y. (2008). *GASSHO1* and *GASSHO2* encoding a putative leucine-rich repeat transmembrane-type receptor kinase are essential for the normal development of the epidermal surface in Arabidopsis embryos. Plant J. 54: 30-42.

Vicente-Carbajosa, J., and Carbonero, P. (2005). Seed maturation: developing an intrusive phase to accomplish a quiescent state. Int. J. Dev. Biol. 49: 645-651.

Vigeolas, H., van Dongen, J.T., Waldeck, P., Hühn, D., and Geigenberger, P. (2003). Lipid storage metabolism is limited by the prevailing low oxygen concentrations within developing seeds of oilseed rape. Plant Physiol. 133: 2048-2060.

Wu, G.-Z., and Xue, H.-W. (2010). Arabidopsis ß-ketoacyl-[acyl carrier protein] synthase I is crucial for fatty acid synthesis and plays a role in chloroplast division and embryo development. Plant Cell 22: 3726-3744.

Xing Q., Creff A., Waters A., Tanaka H., Goodrich J., and Ingram G.C. (2013). ZHOUPI controls embryonic cuticle formation via a signaling pathway involving the subtilisin protease ABNORMAL LEAF-SHAPE1 and the receptor kinases GASSHO1 and GASSHO2. Development 140: 770-779.

Yephremov, A., Wisman, E., Huijser, P., Huijser, C., Wellesen, K., and Saedler, H. (1999). Characterization of the FIDDLEHEAD gene of Arabidopsis reveals a link between adhesion response and cell differentiation in the epidermis. Plant Cell 11: 2197-2201.

FIGURE LEGENDS

Figure 1. Accumulation of ω-9 fatty acids and derivatives in seeds of the *Arabidopsis* accession Col-0.
(A) Time-course analysis of C18:1 and derivatives accumulation in developing seeds. Total fatty acids were analyzed by gas chromatography. Yellow to red stacked bars represent C18:1 and derivatives. Blue segments represent other fatty acids. Values

41

are the means of five replicates performed on batches of 20 to 40 seeds from distinct individuals.

(B) Amounts of C18:1 and derivatives in the different fractions of mature dry seeds. Emb., embryo; Endo., endosperm fraction. Values are the means of five replicates performed on batches of 20 seeds from distinct individuals.

(C-D) Relative proportions of C18:1 and derivatives in the main lipid classes contained in seeds. Lipids were extracted from dry seeds. Concentrations of polar lipids (PLs) and triacylglycerols (TAGs) separated by thin-layer chromatography are expressed on a seed dry weight (DW) basis and indicated in the center of the circular charts (C). The concentration of polyester monomers (D) is expressed on a dry weight basis of delipidated residue (DR). The circular charts represent the fatty acid composition (in Mol %) of each lipid class. Values are the means of five replicates performed on batches of seeds from distinct individuals. DCA, dicarboxylic fatty acid; ωOH, ω-hydroxyl fatty acid.

Figure 2. Patterns of mRNA accumulation among the *AAD* multigene family.

(A-B) Analysis of relative mRNA accumulation of *AADs* was performed in developing seeds (A), in embryo (Emb.) and endosperm fractions (Endo.) dissected from seeds aged 12 or 16 DAA (B). The results obtained are standardized to the constitutive *EF1αA4* (*EF*) gene expression level. Values are the means and SE of three to six replicates carried out on cDNA dilutions obtained from three independent mRNA extractions. DAA, days after anthesis.

Figure 3. Patterns of activity of GUS reporter constructs.

Pattern of activity of the *ProFAB2:FAB2g:uidA*, *ProAAD5:AAD5g:uidA*, *ProAAD1:uidA*, *ProAAD6:uidA*, *ProAAD3:uidA*, *ProAAD2:uidA* and *ProAAD4:uidA* cassettes in young plantlets grown 20 days *in vitro*, in rosette leaves, in cauline leaves, in inflorescences, in flowers, in early maturing embryos harvested 6, 8, 10, or 12 days after anthesis (DAA), and in seed coat plus endosperm fractions from early maturing seeds aged 10 DAA (from left to right). For histochemical detection of GUS activity in vegetative organs and in flowers, tissues were incubated overnight in a buffer containing 0.2 mM each of potassium ferrocyanide and potassium ferricyanide. For seed fractions (embryos or seed coats plus endosperms attached), tissues were incubated 3 h in a buffer containing 2 mM each of potassium ferrocyanide and

potassium ferricyanide. The results for GUS activity were observed on whole-mounted vegetative organs and flowers; microscopy observations of seed fractions were performed using Nomarski optics. Patterns of activity of the *ProAAD5:uidA* and *ProFAB2:uidA* cassettes are displayed in Supplemental Figure 2. Bars = 5 mm (vegetative organs and flowers) or 200 µm (seed fractions).

Figure 4. Functional characterization of *AADs* coding for Δ9 stearoyl-ACP desaturases.

The *fab2-2* mutant was transformed with different *ProFAB2:AADc* constructs. For each *ProFAB2:AADc* cassette tested, three independent transgenic lines (T1-3) were analyzed. Rosette leaves were then subjected to total FA analyses to determine the relative proportion of C18:0 and C16:3. Values are the means and SE of five replicates performed on batches of leaves from distinct plants. Statistical analysis of the data was performed using ANOVA, followed by comparison of means using the Newman-Keuls (SNK) test (P<0.05).

Figure 5. Characterization of *aad* alleles.

(A) Molecular characterization of T-DNA insertion lines. Structure of the *AAD1*, *AAD5*, *AAD6*, and *FAB2* genes showing the position of T-DNA insertions in *aad1-1*, *aad1-3*, *aad5-1*, *aad5-2*, aad5-3, *aad6-1*, *fab2-1*, *fab2-2*, and *fab2-3* are presented. For each T-DNA insertion considered, confirmed flanking sequence tag(s) are anchored in the gene structure and represented by vertical bar(s). Closed boxes represent exons and open boxes untranslated regions (UTRs). Primers used for RT-PCR experiments displayed in (B-D) are indicated by red arrows (see Supplemental Table 2).

(B) Accumulation of *AAD1*, *AAD5*, *AAD6*, and *FAB2* mRNA in the wild type and in knockout mutants was studied by RT-PCR reaction on developing seeds harvested 16 days after anthesis. *EF1αA4* (*EF*) gene expression was used as a constitutive control.

(C) Accumulation of *AAD5* mRNA in the wild type and in the *aad5-1* mutant was first studied by RT-PCR reaction on developing seeds harvested 16 days after anthesis (top right-hand corner). Then, RT-qPCR analyses of transcript abundance in cDNA prepared from maturing seeds or rosette leaves were carried out (bar chart). *EF1αA4* (*EF*) gene expression was used as a constitutive control. Values are the means and

SE of three replicates performed on cDNA dilutions obtained from three independent mRNA extractions. Asterisks indicate significant differences from the wild type according to *t*-test at *** P<0.001 and ** P<0.01, respectively.

(D) Accumulation of *FAB2* mRNA in the wild type and in the *fab2-1* mutant was first studied by RT-PCR reaction on developing seeds harvested 16 days after anthesis (top right-hand corner). Then, RT-qPCR analyses of transcript abundance in cDNA prepared from maturing seeds or rosette leaves were carried out (bar chart). *EF1αA4* (*EF*) gene expression was used as a constitutive control. Values are the means and SE of three replicates performed on cDNA dilutions obtained from three independent mRNA extractions. Asterisks indicate significant differences from the wild type according to *t*-test at *** P<0.001 and * P<0.05, respectively.

(E) Fatty acid composition of mature dry seeds determined by gas chromatography analysis. Yellow to red stacked bars represent C18:1 and derivatives while blue stacked bars represent C18:0 and derivatives. Values are the means and SE of five replicates performed on batches of 20 seeds from five distinct individuals.

Figure 6. Characterization of the embryo-lethal phenotype of *aad5 fab2* mutants.

(A) Fully developed siliques from the wild type (Col-0), *aad5*, *fab2*, and *aad5 fab2/+* mutants were opened and observed using a binocular microscope.

(B) Percentage of aborted seeds per siliques. Values are the means and SE of five replicates. Asterisks indicate significant differences from the wild type according to *t*-test at *** P<0.001.

(C) Genotyping results of self-pollinated *aad5 fab2/+* plants. Asterisks indicate that the observed values and expected values from the specified distribution are statistically different, with an alpha risk of P<0.001.

(D) Observation of seed development. Whole mounts of early developing seeds (4, 6, and 8 days after anthesis) were observed with Nomarski optics.

(E) Longitudinal sections of developing embryos aged 4 and 6 days after anthesis observed by confocal microscopy. e, embryo; i, integument; s, suspensor.

Bars = 1 mm in (A), 50 µm in (D), and 25 µm in (E).

Figure 7. Characterization of the twisted embryos produced by *aad5-1 fab2-2* and *aad1 fab2* mutants.

(A) Pools of mature dry seeds observed under a binocular microscope. White stars denote seeds with a twisted phenotype. Bar = 500 µm.

(B) Dry seeds observed by scanning electron microscopy. Doted arrows denote embryo folding. Bar = 100 µm.

(C) Mature embryos dissected from imbibed seeds and observed by scanning electron microscopy. Bar = 100 µm.

(D) Relative proportion of twisted seeds in different mutant backgrounds. Values are the means and SE of five replicates carried out on batches of 100 seeds from five different plants. Asterisks indicate significant differences from the wild type according to t-test at *** $P<0.001$.

(E-G) Concentrations of several cutin monomers expressed on a dry weight basis of delipidated cotyledons (dry residue, DR) from five-day old seedlings grown under continuous light. Values are the means and SE of five replicates. Asterisks indicate significant differences from the wild type according to t-test at *** $P<0.001$, ** $P<0.01$, and * $P<0.05$, respectively. DCA, dicarboxylic fatty acid; VLCFA, very long-chain fatty acid.

Figure 8. Observation of the developing and germinating embryos of *aad5-1 fab2-2* and *aad1 fab2* mutants.

(A) Observation of embryo elongation and folding in developing seeds. Whole mounts of early maturing seeds (6, 8, and 10 days after anthesis) were observed with Nomarski optics. Isolated arrowheads indicate contact sites between cotyledons and the surrounding tissues in seeds aged 8 days after anthesis. Doted arrows denote embryo folding in seeds aged 10 days after anthesis.

(B) Evaluation of toluidine blue permeability in etiolated seedlings grown for 4 days in the dark.

(C) Evaluation of toluidine blue permeability in seedlings grown for 10 days under day/night alternation.

Bars = 100 µm.

Figure 9. Characterization of oil accumulation in *aad* seeds.

(A) Total fatty acid concentrations in dry seeds determined by gas chromatography. Values are the means and SE of five replicates performed on batches of 20 seeds from five distinct individuals.

(B) Total fatty acid concentrations in the different fractions of mature dry seeds determined by gas chromatography. Emb., embryo; Endo., endosperm fraction. Values are the means and SEs of five replicates performed on batches of 20 seeds from five distinct individuals.

(C) Concentrations of triacylglycerols and polar lipids of dry seeds. The two lipid fractions were separated by this layer chromatography. Values are the means and SE of five replicates performed on batches of 50 seeds from five distinct individuals. Asterisks indicate significant differences from the wild type according to t-test at *** $P<0.001$, ** $P<0.01$, and * $P<0.05$ respectively.

Figure 10. Transcriptional activation of *AA1*, *AAD5*, and *FAB2* by WRINKLED1.

(A-B) Analysis of relative mRNA accumulation of *AADs* was performed in *wri1* mutant seeds aged 10 days after anthesis (A) and in rosette leaves of *WRI1* over expressing lines (B). The results obtained are standardized to the constitutive *EF1αA4* (*EF*) gene expression level. Values are the means and SE of three to six replicates carried out on cDNA dilutions obtained from three independent mRNA extractions. OE, overexpressor; WT, wild type. Asterisks indicate significant differences from the wild type according to t-test at *** $P<0.001$, ** $P<0.01$, and * $P<0.05$, respectively.

(C) Compared analysis of the patterns of activity of GUS reporter constructs in populations of maturing embryos from hemizygous *wri1-3*/+ lines segregating the T-DNA causing the *wri1-3* mutation. For each GUS reporter gene construct analyzed, two independent transformants were crossed with the *wri1-3* mutant. Their progeny (T0) was propagated. Then, *wri1-3*/+ hemizygous plants were selected by PCR screening among the T1 lines. Homozygosity of the GUS reporter cassette in the selected lines was assessed on the basis of segregation analyses carried out on hygromycin with their progeny. Seeds from the lines thus obtained were excised from maturing siliques and sorted according to their wrinkled (*wri1*) or wild-type phenotype (WT). Embryos were then dissected and incubated at room temperature for 2 h (*FAB2* reporter construct) or 3 h (*AAD1* and *AAD5* reporter constructs) in a buffer containing 2 mM each of potassium ferrocyanide and potassium ferricyanide. Microscopy observations of embryos were performed using Nomarski optics. The proportion of stained embryos in each category is indicated on the figure (n = total number of embryos observed).

(D) Transactivation assay in leaves of *Nicotiana benthamiana*. GUS reporter gene constructs alone or in combination with a vector allowing the expression of *WRI1* or *MYB115* (negative control) were co-infiltrated in young leaves of *N. benthamiana* with a vector allowing the production of the p19 protein of tomato bushy stunt virus (TBSV) that prevents the onset of post-transcriptional gene silencing (Shamloul et al., 2014). Leaf discs were assayed for GUS activity three days after infiltration. Tissues were incubated 3 h in a buffer containing 2 mM each of potassium ferrocyanide and potassium ferricyanide. Representative discs (diameter = 0.8 cm) are presented.

(E) Analysis of WRI binding to the promoters of *BCCP2*, *AAD1*, *AAD5* and *FAB2* in yeast one-hybrid experiments. Yeast strains containing the *HIS3* reporter gene under the control of either the *BCCP2* (positive control), *AAD1*, *AAD5* or *FAB2* promoter were transformed with either the empty pDEST22 expression vector or with a version of this vector allowing the expression of *WRI1* before being plated on appropriate media to maintain the expression of the vectors (SD-U-W) and to test the activation of the *HIS3* reporter gene (SD-U-W-H). Data presented are representative from the results obtained for five independent colonies. SD, synthetic drop-out medium.

(F) Binding of WRI1 to the proximal upstream region of *FAB2*. Electrophoretic mobility shift assay (EMSA) of a probe covering a region from -800 to -721 upstream from the ATG codon of *FAB2* (see Supplemental Figure 3). LEAFY COTYLEDON2 (LEC2) was used as a negative control. Competition of WRI1 binding was carried out in the presence of 100-, 500-, and 1,000-fold amounts of the unlabeled *ProFAB2* fragment. Position of free probe (open arrowhead) and the shifted bands (closed arrowhead) are indicated.

Figure 11. Biosynthesis and fate of monounsaturated fatty acids in developing seeds of *Arabidopsis*.

The WRINKLED1 (WRI1) transcription factor directly enhances the transcription of three Δ9 stearoyl-ACP desaturase (SAD)-coding genes, namely *AAD1*, *AAD5*, and *FAB2*, in zygotic tissues of early-maturing seeds. Endosperm-specific induction of *AAD2* and *AAD3*, that encode Δ9 palmitoyl-ACP desaturases (PADs), is triggered by MYB118 and, to a lesser extent, by MYB115 (not presented). In the developing embryo, ω-9 monounsaturated fatty acids (MUFAs) are essential for the elaboration of membrane lipids, surface lipids, and storage lipids (triacyglycerols). The cuticle deposited at the surface of the embryo, together with the embryo sheath, plays a key

47

role in embryo-endosperm separation and correct embryo elongation during early-maturation. Triacylglycerols stored in the embryo during the maturation phase comprise up to 85 mol % of ω-9 MUFAs and their polyunsaturated derivatives (PUFAs). In the endosperm, ω-9 MUFAs are used for the production of membrane lipids and storage lipids. Due to the concomitant transcriptional activation of SAD- and PAD-coding genes in the maturing endosperm, triacyglycerols accumulated in this seed compartment comprise almost equivalent proportions of ω-7 and ω-9 MUFAs. Recent studies suggest that the cuticle separating endosperm cells from the inner cell layer of the seed coat is of maternal origin (Loubéry et, 2018). The synthesis of this cuticle layer by cells of the seed coat was therefore omitted.

Supplemental Figure 1. Complementary information for the characterization of the patterns of mRNA accumulation among the *AAD* family.

Analysis of relative mRNA accumulation of *AADs* was performed in different plant organs. The results obtained are standardized to the constitutive *EF1αA4* (*EF*) gene expression level. Values are the means and SE of three to six replicates carried out on cDNA dilutions obtained from three independent mRNA extractions. Cl, cauline leaves; Fl, flowers; ND, not detected; Rl, rosette leaves; Ro, roots; St, stems.

Supplemental Figure 2. Complementary information for the pattern of activity of GUS reporter constructs.

(A) Pattern of activity of the *ProAAD2:uidA* cassette in stipules of rosette leaves.

(B) Pattern of activity of the *ProAAD3:uidA* cassette in root tips.

(C-E) Pattern of activity of the *ProAAD5:uidA* (C), *ProFAB2_{1kb}:uidA* (D), and *ProFAB2_{1.6kb}:uidA* cassettes (E) in young plantlets grown 20 days *in vitro*, rosette leaves, cauline leaves, inflorescences, flowers, early maturing embryos harvested 6, 8, 10, or 12 days after anthesis, and seed coat plus endosperm fractions from early maturing seeds aged 10 days after anthesis (from left to right).

For histochemical detection of GUS activity in vegetative organs and in flowers, tissues were incubated overnight in a buffer containing 0.2 mM each of potassium ferrocyanide and potassium ferricyanide. For seed fractions (embryos or seed coats plus endosperms attached), tissues were incubated 3 h in a buffer containing 2 mM each of potassium ferrocyanide and potassium ferricyanide. The results for GUS activity were observed on whole-mounted vegetative organs and flowers; microscopy

observations of seed fractions were performed using Nomarski optics. Bars = 100 µm in (A) and (B), 5 mm in (C-E) (plantlets and plant organs), and 200 µm in (C-E) (seed fractions).

Supplemental Figure 3. Complementary information for the sequences of *Arabidopsis* AADs.

Alignment of amino acid sequences of AAD1, AAD5, AAD6, FAB2, and the Δ9 SAD from *Ricinus communis* was generated by the MUSCLE program (www.phylogeny.fr). Conserved amino acid residues lining the bottom part of the substrate channel of the enzymes are colored in red and indicated with asterisks.

Supplemental Figure 4. Complementary information for the characterization of *fab2* mutants expressing *ProFAB2:AADc* constructs.

RT-qPCR analysis of transcript abundance in cDNA prepared from rosette leaves were first carried out to assess efficient overexpression of the transgenes. Values are the means and SE of three to ten replicates carried out on cDNA dilutions obtained from three to five independent mRNA extractions. Statistical analysis of the data was performed using ANOVA, followed by comparison of means using the Newman-Keuls (SNK) test ($P<0.05$).

Supplemental Figure 5. Phenotype of *aad5/+ fab2* mutants.

Wild-type (Col-0) and mutant plants were photographed six weeks after germination, prior to DNA extractions and subsequent genotyping carried out by PCR. Bars = 1 cm.

Supplemental Figure 6. Complementary information for the biochemical characterization of seed fractions from a subset of *aad* mutants.

Total fatty acid compositions in the different fractions of mature dry seeds were determined by gas chromatography. Emb., embryo; Endo., endosperm fraction. Values are the means and SEs of five replicates performed on batches of 20 seeds from distinct individuals. Asterisks indicate significant differences from the wild type according to *t*-test at *** $P<0.001$.

Supplemental Figure 7. Complementary information for the biochemical characterization of dry seeds from a subset of *aad* mutants.

(A) Total fatty acid composition of polar lipids (PLs) and triacylglycerols (TAGs) separated by thin-layer chromatography. Values are the means and SE of five replicates performed on batches of seeds from distinct individuals.

(B) Characterization of the polyester monomer composition. Values are the means and SE of three to four replicates performed on batches of seeds from distinct individuals. DCA, dicarboxylic fatty acid; OH, 1-fatty alcohol; ωOH, ω-hydroxyl fatty acid.

C18:0 and derivatives are presented on the upper row of graphs, whereas C18:1 and derivatives are presented on the lower row of graphs. Asterisks indicate significant differences from the wild type according to *t*-test at *** $P<0.001$, ** $P<0.01$, and * $P<0.05$ respectively.

Supplemental Figure 8. Test of genetic transmission of *aad5* and *fab2* gametophytes.

(A) Genotyping results of reciprocal crossing between *aad5-3 fab2-2*/+ and wild-type plants.

(B) Genotyping results of reciprocal crossing between *aad5-2 fab2-3*/+ and wild-type plants.

(C) Light micrograph of mature anther from flower of wild type plants and *aad5 fab2*/+ mutants stained with Alexander's solution. Bar = 200 µm.

(D) Whole mounts of unfertilized ovules within carpels of wild type plants and *aad5 fab2*/+ mutants observed with Nomarski optics. Bar = 200 µm.

Supplemental Figure 9. Rescue of the lethal phenotype of *aad5-2 fab2-3* mutants with either *AAD5* or *FAB2* gene sequence.

(A) Cassettes encompassing either *AAD5* or *FAB2* gene used to rescue the double mutant. Red arrows indicate primers used for PCR experiments displayed in (D).

(B) Structure of the *AAD5* and *FAB2* genes showing the position of T-DNA insertions in *aad5-2* and *fab2-3*. Closed boxes represent exons and open boxes untranslated regions (UTRs). Red arrows indicate primers used for PCR experiments displayed in (D).

(C) Sequence of the primers used to genotype plant material in this experiment.

(D) PCR genotyping of the transformants and control plants. WT, wild type.

Supplemental Figure 10. Phenotype of the *aad5-2 fab2-3* double mutants rescued with either *AAD5* or *FAB2* gene sequence.

(A) Rosettes photographed 26 days after germination, prior to fresh weight measurements and fatty acid extractions. Bar = 1 cm.

(B) Rosette fresh weight (FW). Values are the means and SE of ten measurements. Statistical analysis of the data was performed using ANOVA, followed by comparison of means using the Newman-Keuls (SNK) test (P<0.05).

(C) Relative proportion of C18:0 and C16:3 among total fatty acids extracted from rosette leaves. Values are the means and SE of five replicates performed on batches of leaves from distinct plants. Statistical analysis of the data was performed using ANOVA, followed by comparison of means using the Newman-Keuls (SNK) test (P<0.05).

Supplemental Figure 11. Complementary information for the characterization of mutants producing twisted embryos.

(A) Pools of mature dry seeds observed under a binocular microscope. Bar = 500 μm.

(B) Dry seeds observed by scanning electron microscopy. Doted arrows denote embryo folding. Bar = 100 μm.

(C) Mature embryos dissected from imbibed seeds and observed by scanning electron microscopy. Bar = 100 μm.

(D) Test of the causal influence of the maternal genotype on the twisted phenotype of seeds. The *aad5-1 fab2-2* and *aad1 fab2* mutants were either self-pollinated or subjected to reciprocal crosses with the wild type. The proportion of twisted seeds in their progeny was then determined. The number of seeds observed is indicated for each cross.

Supplemental Figure 12. Complementary information for the characterization of the developing and germinating embryos of *aad5-1 fab2-2* and *aad1 fab2* mutants.

(A) Observation of embryo elongation and folding in developing seeds. Whole mounts of early maturing seeds (6, 8, and 10 days after anthesis) were observed with Nomarski optics. Isolated arrowheads indicate contact sites between cotyledons and

the surrounding tissues in seeds aged 8 days after anthesis. Doted arrows denote embryo folding in seeds aged 10 days after anthesis.

(B) Evaluation of toluidine blue permeability in etiolated seedlings grown for four days in the dark.

(C) Evaluation of toluidine blue permeability in seedlings grown for 10 days under day/night alternation.

Bars = 100 μm.

Supplemental Figure 13. Complementary information for the characterization of the twisted embryos produced by *aad5-1 fab2-2* and *aad1 fab2* mutants.

(A) Confocal images of Auramine-O stained cuticle in cotyledons of wild-type and mutant plantlets germinated 7 days under continuous light. Auramine 0 (green), chlorophyll autofluorescence (red). Bar = 100 μm.

(B) Total concentrations of cutin monomers expressed on a dry weight basis of delipidated cotyledons (dry residue, DR) from five-day old seedlings. Values are the means and SE of five replicates. Asterisks indicate significant differences from the wild type according to *t*-test at * P<0.05.

(C) Complementary details regarding the composition of cutin monomers expressed on a dry weight basis of delipidated cotyledons from five-day old seedlings. Values are the means and SE of five replicates. DCA, dicarboxylic fatty acid; ωOH, ω-hydroxyl fatty acid.

Supplemental Figure 14. Promoter sequences of the three *AAD* genes induced by WRINKLED1.

ATG translational start codons are highlighted in blue whereas the *cis*-regulatory elements putatively bound by WRINKLED1 are highlighted in yellow. Nucleotides colored in red correspond to the conserved residues of the AW-box as defined by Maeo and coworkers (2009). The underlined sequence corresponds to the DNA fragment used for electrophoretic mobility shift assays.

Supplemental Figure 15. Complementary information for the tissue-specific expression of SAD-coding genes in the seed.

A selection of previously published transcriptomic data is displayed that precise the expression patterns of the four SAD-coding genes in the embryo proper at very early stages of development (A) and in different tissues of a torpedo-shape embryos (B).
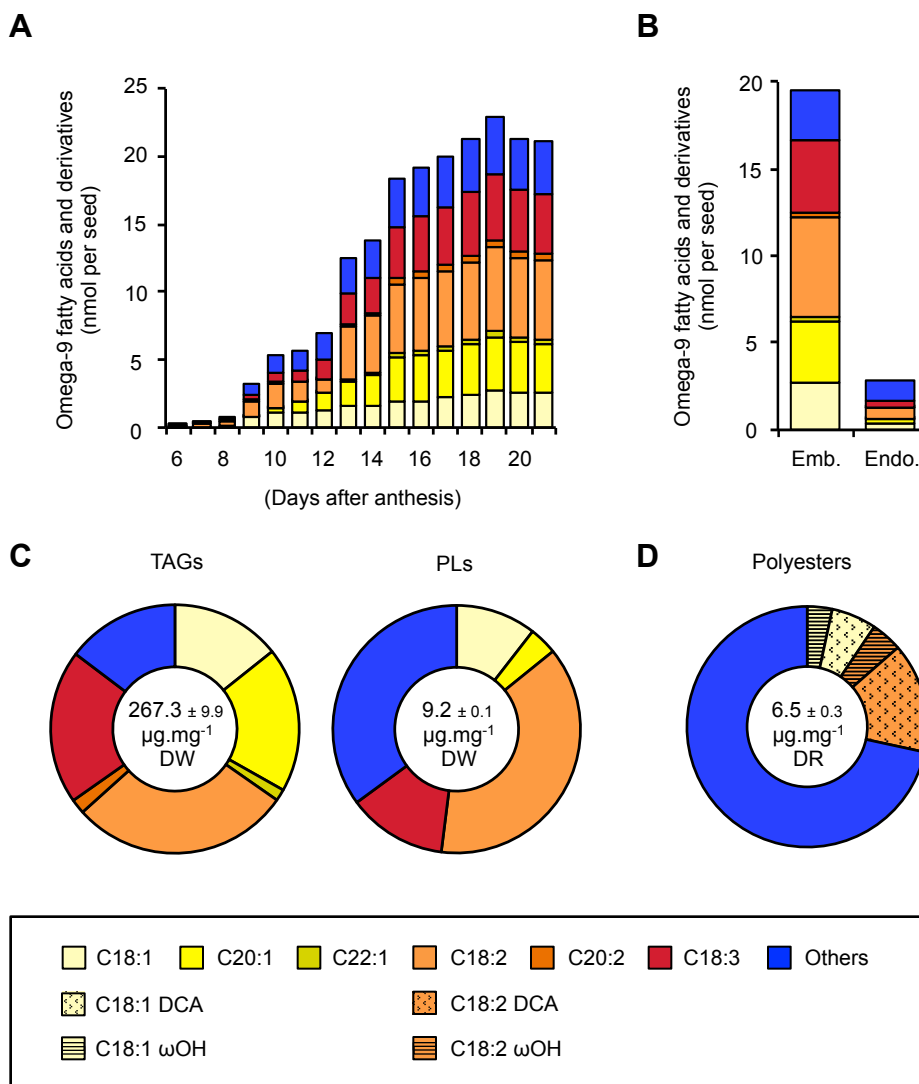
Figure 1. Accumulation of ω-9 fatty acids and derivatives in seeds of the *Arabidopsis* accession Col-0.
(A) Time-course analysis of C18:1 and derivatives accumulation in developing seeds. Total fatty acids were analyzed by gas chromatography. Yellow to red stacked bars represent C18:1 and derivatives. Blue segments represent other fatty acids. Values are the means of five replicates performed on batches of 20 to 40 seeds from distinct individuals.
(B) Amounts of C18:1 and derivatives in the different fractions of mature dry seeds. Emb., embryo; Endo., endosperm fraction. Values are the means of five replicates performed on batches of 20 seeds from distinct individuals.
(C-D) Relative proportions of C18:1 and derivatives in the main lipid classes contained in seeds. Lipids were extracted from dry seeds. Concentrations of polar lipids (PLs) and triacylglycerols (TAGs) separated by thin-layer chromatography are expressed on a seed dry weight (DW) basis and indicated in the center of the circular charts (C). The concentration of polyester monomers (D) is expressed on a dry weight basis of delipidated residue (DR). The circular charts represent the fatty acid composition (in Mol %) of each lipid class. Values are the means of five replicates performed on batches of seeds from distinct individuals. DCA, dicarboxylic fatty acid; ωOH, ω-hydroxyl fatty acid.
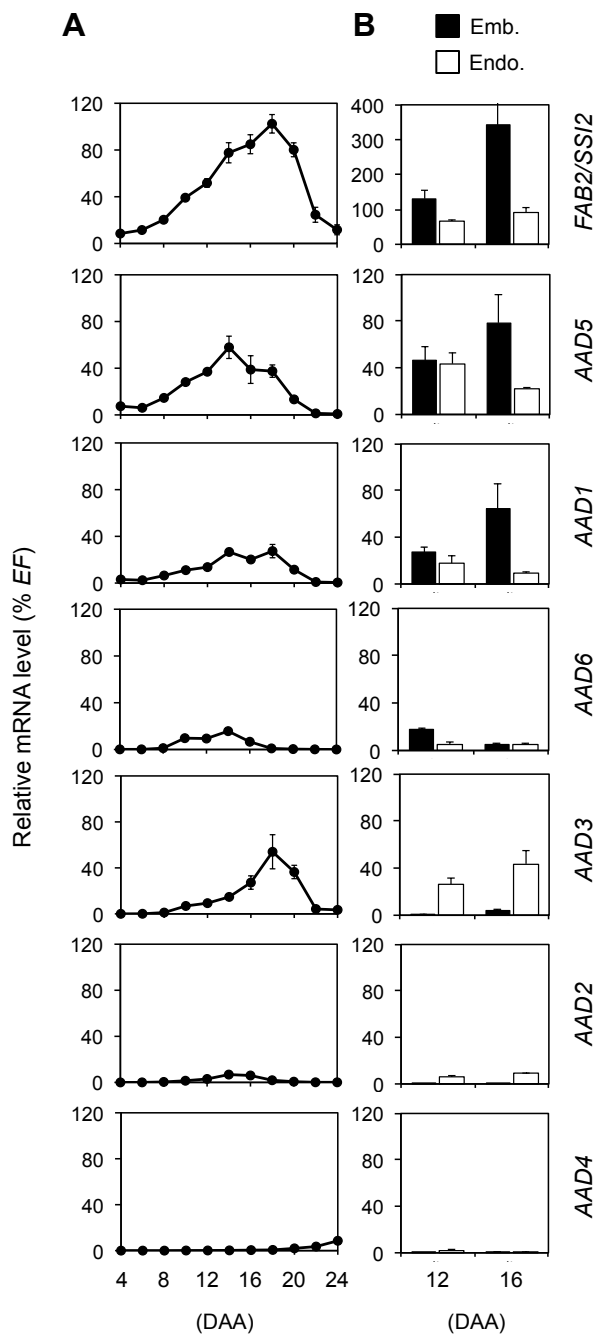
Figure 2. Patterns of mRNA accumulation among the *AAD* multigene family. (A-B) Analysis of relative mRNA accumulation of *AADs* was performed in developing seeds (A), in embryo (Emb.) and endosperm fractions (Endo.) dissected from seeds aged 12 or 16 DAA (B). The results obtained are standardized to the constitutive *EF1αA4* (*EF*) gene expression level. Values are the means and SE of three to six replicates carried out on cDNA dilutions obtained from three independent mRNA extractions. DAA, days after anthesis.

Figure 3. Patterns of activity of GUS reporter constructs.
Pattern of activity of the *ProFAB2:FAB2g:uidA*, *ProAAD5:AAD5g:uidA*, *ProAAD1:uidA*, *ProAAD6:uidA*, *ProAAD3:uidA*, *ProAAD2:uidA* and *ProAAD4:uidA* cassettes in young plantlets grown 20 days *in vitro*, in rosette leaves, in cauline leaves, in inflorescences, in flowers, in early maturing embryos harvested 6, 8, 10, or 12 days after anthesis (DAA), and in seed coat plus endosperm fractions from early maturing seeds aged 10 DAA (from left to right). For histochemical detection of GUS activity in vegetative organs and in flowers, tissues were incubated overnight in a buffer containing 0.2 mM each of potassium ferrocyanide and potassium ferricyanide. For seed fractions (embryos or seed coats plus endosperms attached), tissues were incubated 3 h in a buffer containing 2 mM each of potassium ferrocyanide and potassium ferricyanide. The results for GUS activity were observed on whole-mounted vegetative organs and flowers; microscopy observations of seed fractions were performed using Nomarski optics. Patterns of activity of the *ProAAD5:uidA* and *ProFAB2:uidA* cassettes are displayed in Supplemental Figure 2. Bars = 5 mm (vegetative organs and flowers) or 200 µm (seed fractions).
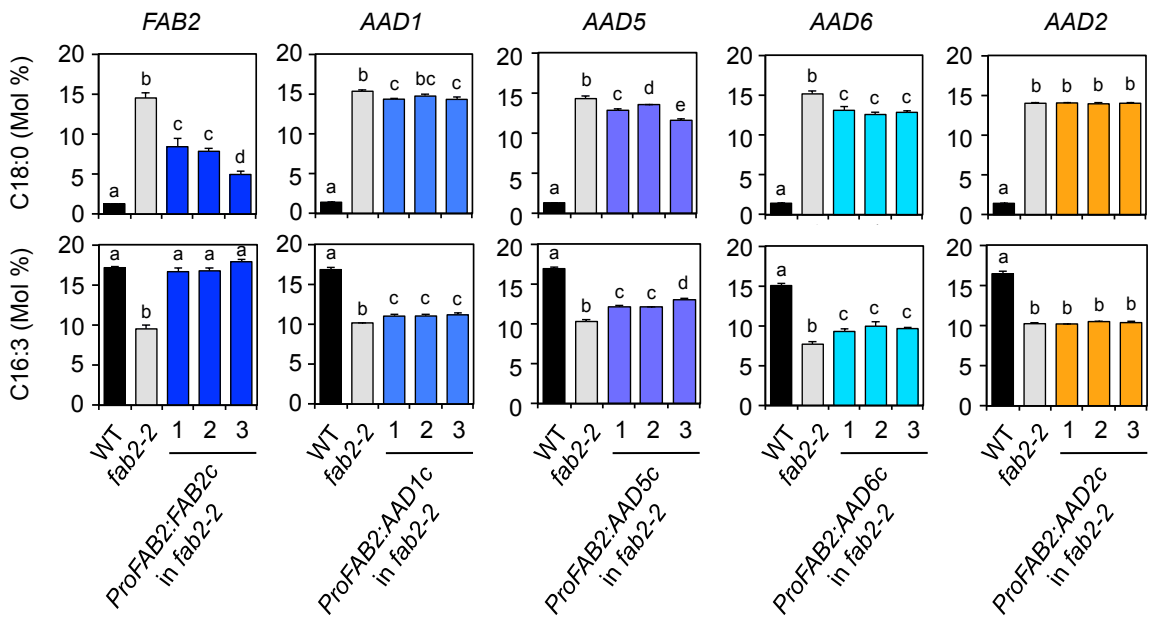
Figure 4. Functional characterization of *AADs* coding for Δ9 stearoyl-ACP desaturases.
The *fab2-2* mutant was transformed with different *ProFAB2:AADc* constructs. For each *ProFAB2:AADc* cassette tested, three independent transgenic lines (T1-3) were analyzed. Rosette leaves were then subjected to total FA analyses to determine the relative proportion of C18:0 and C16:3. Values are the means and SE of five replicates performed on batches of leaves from distinct plants. Statistical analysis of the data was performed using ANOVA, followed by comparison of means using the Newman-Keuls (SNK) test (P<0.05).

A

AAD1 - At5g16240

ATG

aad1-1   aad1-3

AAD5 - At3g02630

aad5-1   ATG   aad5-3 aad5-2

AAD6 – At1g43800

ATG
aad6-1

FAB2 – At2g43710

fab2-1   ATG   fab2-3   fab2-2

B

AAD1
EF
WT aad1-1 aad1-3

AAD5
EF
WT aad5-3 aad5-2

AAD6
EF
WT aad6-1

FAB2
EF
WT fab2-3 fab2-2

C

AAD5
EF
WT aad5-1

Relative mRNA level (% *EF*)

***

**

Seeds   Leaves

D

FAB2
EF
WT fab2-1

Relative mRNA level (% *EF*)

***

*

Seeds   Leaves

E

□ C18:1 □ C20:1 □ C22:1 □ C18:2 □ C20:2 ■ C18:3 □ C18:0 ■ C20:0 ■ C22:0

Fatty acid composition (Mol %)

WT, aad6-1, aad1-1, aad1-3, aad5-1, aad1-1 aad6-1, aad5-2, aad5-3, aad1-3 aad6-1, aad5-3 aad6-1, aad5-2 aad6-1, aad1-1 aad5-2, aad1-3 aad5-3, aad1-1 aad5-2 aad6-1, fab2-1, aad1-3 aad5-3 aad6-1, fab2-3, fab2-2, aad6-1 fab2-3, aad6-1 fab2-2, aad5-1 fab2-2, aad5-2 fab2-1, aad5-3 fab2-2, aad1-3 fab2-2, aad1-1 fab2-2, aad1-3 aad5-3 fab2-3, aad1-1 fab2-3, aad1-1 aad6-1 fab2-3, aad1-3 aad5-3 fab2-1, aad1-1 aad5-3 aad6-1 fab2-2, aad1-3 aad5-2 fab2-1, aad1-1 aad5-2 fab2-1, aad1-3 aad5-3 aad6-1 fab2-1, aad1-1 aad5-2 aad6-1 fab2-1

Figure 5. Characterization of *aad* alleles.

(A) Molecular characterization of T-DNA insertion lines. Structure of the *AAD1*, *AAD5*, *AAD6*, and *FAB2* genes showing the position of T-DNA insertions in *aad1-1*, *aad1-3*, *aad5-1*, *aad5-2*, aad5-3, *aad6-1*, *fab2-1*, *fab2-2*, and *fab2-3* are presented. For each T-DNA insertion considered, confirmed flanking sequence tag(s) are anchored in the gene structure and represented by vertical bar(s). Closed boxes represent exons and open boxes untranslated regions (UTRs). Primers used for RT-PCR experiments displayed in (B-D) are indicated by red arrows (see Supplemental Table 2).

(B) Accumulation of *AAD1*, *AAD5*, *AAD6*, and *FAB2* mRNA in the wild type and in knockout mutants was studied by RT-PCR reaction on developing seeds harvested 16 days after anthesis. *EF1αA4* (*EF*) gene expression was used as a constitutive control.

(C) Accumulation of *AAD5* mRNA in the wild type and in the *aad5-1* mutant was first studied by RT-PCR reaction on developing seeds harvested 16 days after anthesis (top right-hand corner). Then, RT-qPCR analyses of transcript abundance in cDNA prepared from maturing seeds or rosette leaves were carried out (bar chart). *EF1αA4* (*EF*) gene expression was used as a constitutive control. Values are the means and SE of three replicates performed on cDNA dilutions obtained from three independent mRNA extractions. Asterisks indicate significant differences from the wild type according to *t*-test at *** P<0.001 and ** P<0.01, respectively.

(D) Accumulation of *FAB2* mRNA in the wild type and in the *fab2-1* mutant was first studied by RT-PCR reaction on developing seeds harvested 16 days after anthesis (top right-hand corner). Then, RT-qPCR analyses of transcript abundance in cDNA prepared from maturing seeds or rosette leaves were carried out (bar chart). *EF1αA4* (*EF*) gene expression was used as a constitutive control. Values are the means and SE of three replicates performed on cDNA dilutions obtained from three independent mRNA extractions. Asterisks indicate significant differences from the wild type according to *t*-test at *** P<0.001 and * P<0.05, respectively.

(E) Fatty acid composition of mature dry seeds determined by gas chromatography analysis. Yellow to red stacked bars represent C18:1 and derivatives while blue stacked bars represent C18:0 and derivatives. Values are the means and SE of five replicates performed on batches of 20 seeds from five distinct individuals.
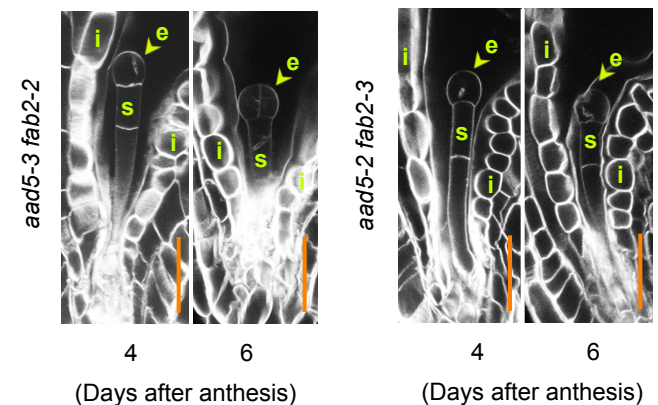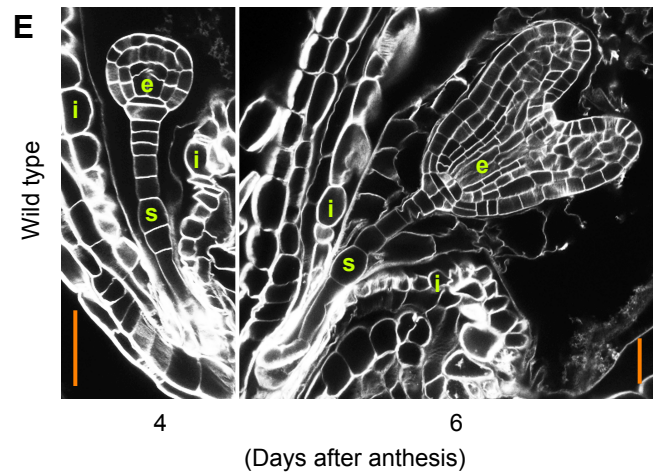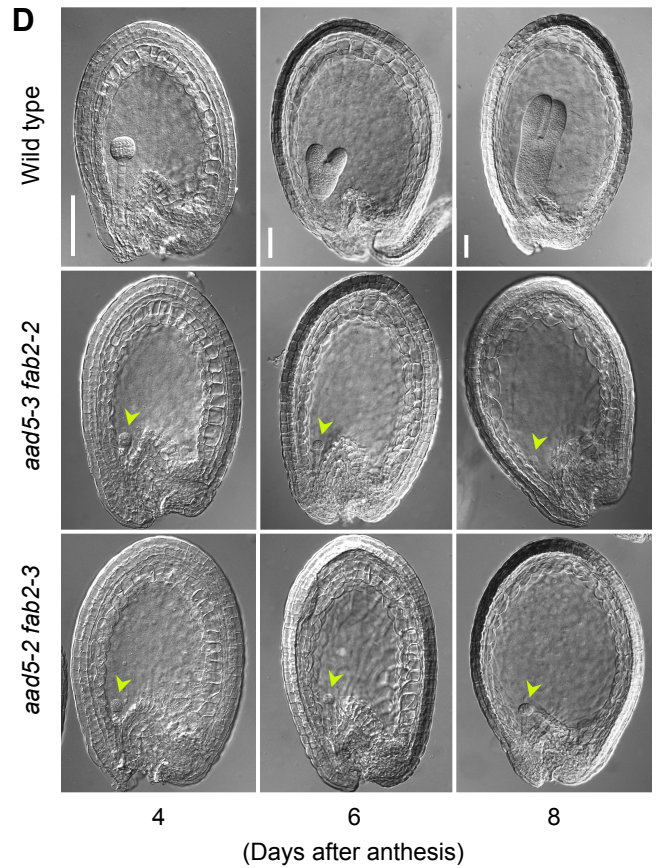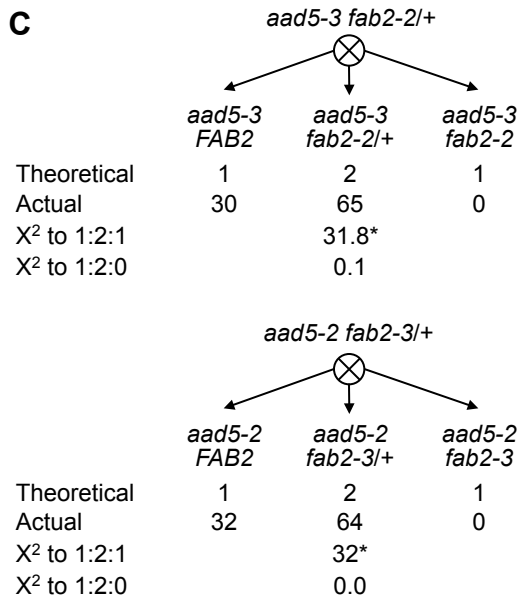
A Wild type, aad5-3, aad5-2, fab2-3, fab2-2, aad5-1 fab2-2/+, aad5-2 fab2-1/+

B

C

aad5-3 fab2-2/+ ⊗

	aad5-3 FAB2	aad5-3 fab2-2/+	aad5-3 fab2-2
Theoretical	1	2	1
Actual	30	65	0
X² to 1:2:1		31.8*	
X² to 1:2:0		0.1	

aad5-2 fab2-3/+ ⊗

	aad5-2 FAB2	aad5-2 fab2-3/+	aad5-2 fab2-3
Theoretical	1	2	1
Actual	32	64	0
X² to 1:2:1		32*	
X² to 1:2:0		0.0	

D

Wild type, aad5-3 fab2-2, aad5-2 fab2-3

4   6   8

(Days after anthesis)

E

Wild type

4   6

(Days after anthesis)

aad5-3 fab2-2   aad5-2 fab2-3

4   6   4   6

(Days after anthesis)   (Days after anthesis)

Figure 6. Characterization of the embryo-lethal phenotype of *aad5 fab2* mutants.

(A) Fully developed siliques from the wild type (Col-0), *aad5*, *fab2*, and *aad5 fab2/+* mutants were opened and observed using a binocular microscope.

(B) Percentage of aborted seeds per siliques. Values are the means and SE of five replicates. Asterisks indicate significant differences from the wild type according to *t*-test at *** $P<0.001$.

(C) Genotyping results of self-pollinated *aad5 fab2/+* plants. Asterisks indicate that the observed values and expected values from the specified distribution are statistically different, with an alpha risk of $P<0.001$.

(D) Observation of seed development. Whole mounts of early developing seeds (4, 6, and 8 days after anthesis) were observed with Nomarski optics.

(E) Longitudinal sections of developing embryos aged 4 and 6 days after anthesis observed by confocal microscopy. e, embryo; i, integument; s, suspensor.

Bars = 1 mm in (A), 50 μm in (D), and 25 μm in (E).

A Wild type | *aad5-1 fab2-2* | *aad1-1 fab2-3* | *aad1-3 fab2-2*

D Twisted seeds (%)

E C18:1 DCA (µg.mg⁻¹ DR)

F C18:0 (µg.mg⁻¹ DR)

G VLCFA (µg.mg⁻¹ DR)

C26:0
C24:0
C22:0
C20:0

Wild type
aad1-1
aad1-3
aad5-1
fab2-3
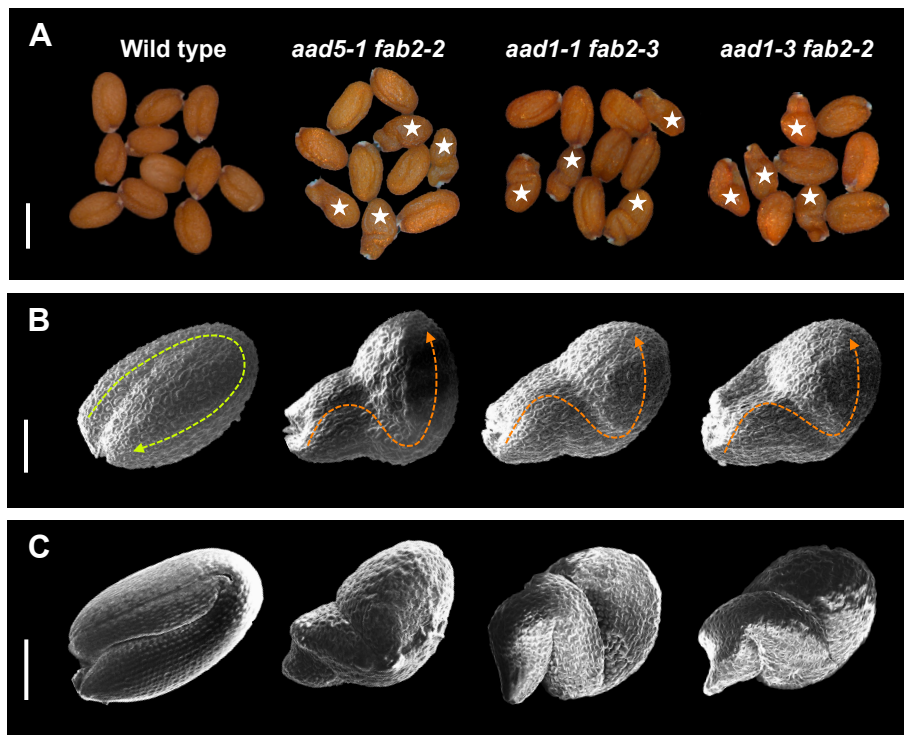*fab2-2*
aad5-1 fab2-2
aad1-1 fab2-3
aad1-3 fab2-2

Figure 7. Characterization of the twisted embryos produced by *aad5-1 fab2-2* and *aad1 fab2* mutants.

(A) Pools of mature dry seeds observed under a binocular microscope. White stars denote seeds with a twisted phenotype. Bar = 500 µm.

(B) Dry seeds observed by scanning electron microscopy. Doted arrows denote embryo folding. Bar = 100 µm.

(C) Mature embryos dissected from imbibed seeds and observed by scanning electron microscopy. Bar = 100 µm.

(D) Relative proportion of twisted seeds in different mutant backgrounds. Values are the means and SE of five replicates carried out on batches of 100 seeds from five different plants. Asterisks indicate significant differences from the wild type according to *t*-test at *** $P<0.001$.

(E-G) Concentrations of several cutin monomers expressed on a dry weight basis of delipidated cotyledons (dry residue, DR) from five-day old seedlings grown under continuous light. Values are the means and SE of five replicates. Asterisks indicate significant differences from the wild type according to *t*-test at *** $P<0.001$, ** $P<0.01$, and * $P<0.05$, respectively. DCA, dicarboxylic fatty acid; VLCFA, very long-chain fatty acid.
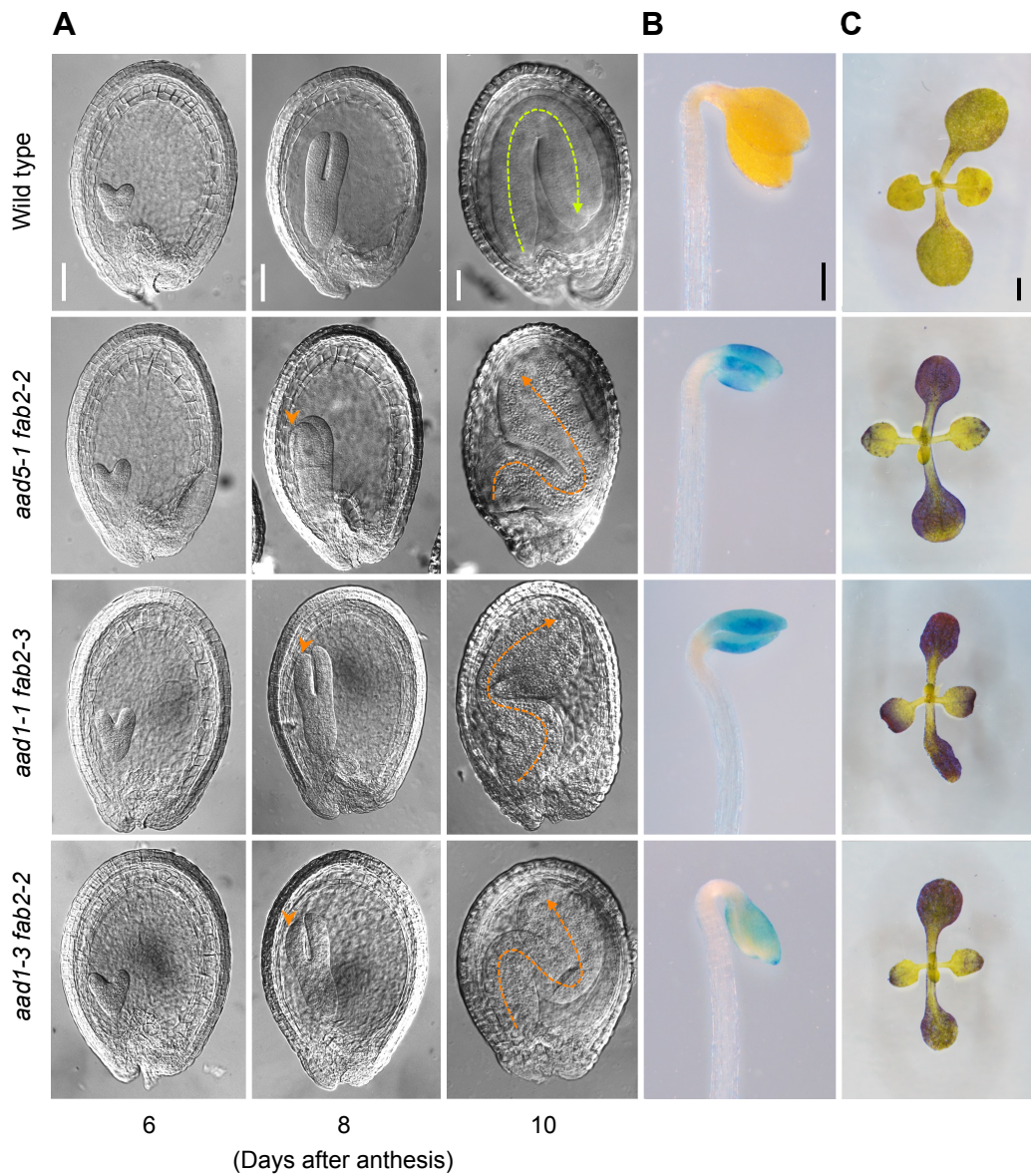
Figure 8. Observation of the developing and germinating embryos of *aad5-1 fab2-2* and *aad1 fab2* mutants.

(A) Observation of embryo elongation and folding in developing seeds. Whole mounts of early maturing seeds (6, 8, and 10 days after anthesis) were observed with Nomarski optics. Isolated arrowheads indicate contact sites between cotyledons and the surrounding tissues in seeds aged 8 days after anthesis. Doted arrows denote embryo folding in seeds aged 10 days after anthesis.

(B) Evaluation of toluidine blue permeability in etiolated seedlings grown for 4 days in the dark.

(C) Evaluation of toluidine blue permeability in seedlings grown for 10 days under day/night alternation.

Bars = 100 µm.

Figure 9. Characterization of oil accumulation in *aad* seeds.
(A) Total fatty acid concentrations in dry seeds determined by gas chromatography. Values are the means and SE of five replicates performed on batches of 20 seeds from five distinct individuals.
(B) Total fatty acid concentrations in the different fractions of mature dry seeds determined by gas chromatography. Emb., embryo; Endo., endosperm fraction. Values are the means and SEs of five replicates performed on batches of 20 seeds from five distinct individuals.
(C) Concentrations of triacylglycerols and polar lipids of dry seeds. The two lipid fractions were separated by this layer chromatography. Values are the means and SE of five replicates performed on batches of 50 seeds from five distinct individuals.
Asterisks indicate significant differences from the wild type according to *t*-test at *** P<0.001, ** P<0.01, and * P<0.05 respectively.
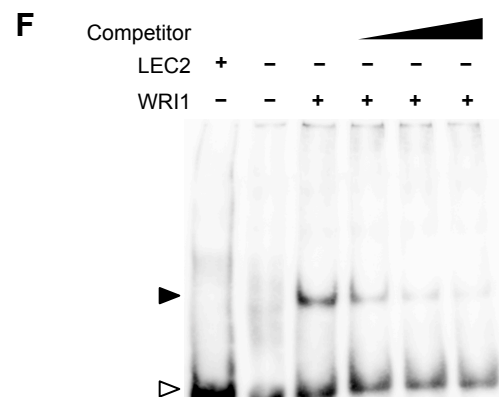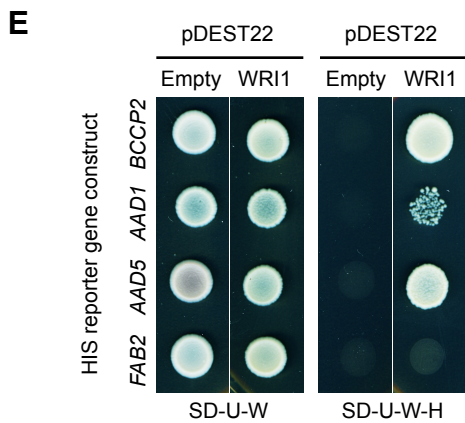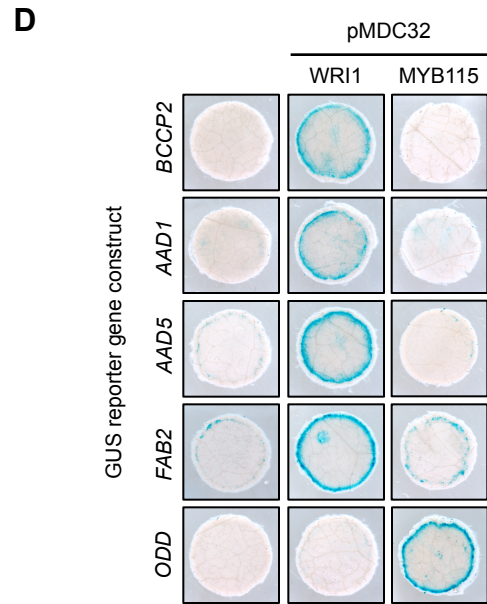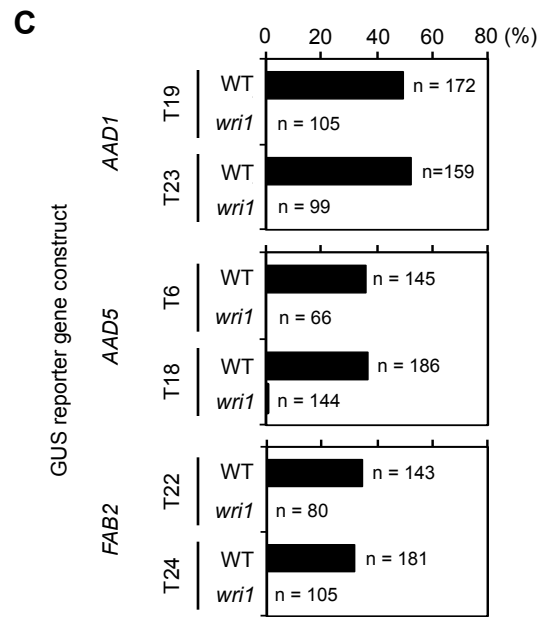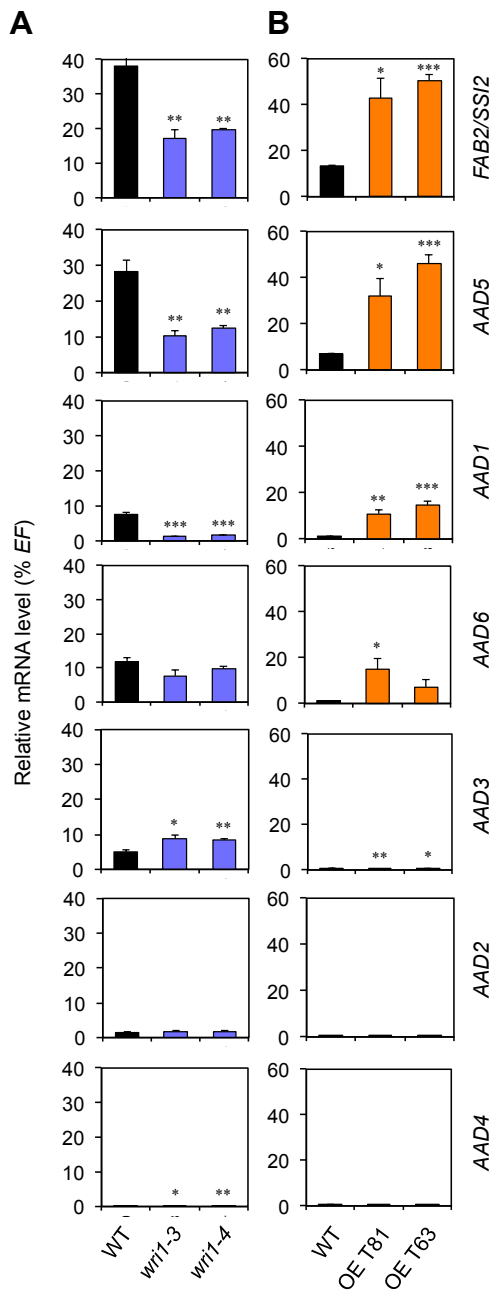
Figure 10. Transcriptional activation of *AA1*, *AAD5*, and *FAB2* by WRINKLED1.
(A-B) Analysis of relative mRNA accumulation of *AADs* was performed in *wri1* mutant seeds aged 10 days after anthesis (A) and in rosette leaves of *WRI1* over expressing lines (B). The results obtained are standardized to the constitutive *EF1αA4* (*EF*) gene expression level. Values are the means and SE of three to six replicates carried out on cDNA dilutions obtained from three independent mRNA extractions. OE, overexpressor; WT, wild type. Asterisks indicate significant differences from the wild type according to *t*-test at *** $P<0.001$, ** $P<0.01$, and * $P<0.05$, respectively.
(C) Compared analysis of the patterns of activity of GUS reporter constructs in populations of maturing embryos from hemizygous *wri1-3*/+ lines segregating the T-DNA causing the *wri1-3* mutation. For each GUS reporter gene construct analyzed, two independent transformants were crossed with the *wri1-3* mutant. Their progeny (T0) was propagated. Then, *wri1-3*/+ hemizygous plants were selected by PCR screening among the T1 lines. Homozygosity of the GUS reporter cassette in the selected lines was assessed on the basis of segregation analyses carried out on hygromycin with their progeny. Seeds from the lines thus obtained were excised from maturing siliques and sorted according to their wrinkled (*wri1*) or wild-type phenotype (WT). Embryos were then dissected and incubated at room temperature for 2 h (*FAB2* reporter construct) or 3 h (*AAD1* and *AAD5* reporter constructs) in a buffer containing 2 mM each of potassium ferrocyanide and potassium ferricyanide. Microscopy observations of embryos were performed using Nomarski optics. The proportion of stained embryos in each category is indicated on the figure (n = total number of embryos observed).
(D) Transactivation assay in leaves of *Nicotiana benthamiana*. GUS reporter gene constructs alone or in combination with a vector allowing the expression of *WRI1* or *MYB115* (negative control) were co-infiltrated in young leaves of *N. benthamiana* with a vector allowing the production of the p19 protein of tomato bushy stunt virus (TBSV) that prevents the onset of post-transcriptional gene silencing (Shamloul et al., 2014). Leaf discs were assayed for GUS activity three days after infiltration. Tissues were incubated 3 h in a buffer containing 2 mM each of potassium ferrocyanide and potassium ferricyanide. Representative discs (diameter = 0.8 cm) are presented.
(E) Analysis of WRI binding to the promoters of *BCCP2*, *AAD1*, *AAD5* and *FAB2* in yeast one-hybrid experiments. Yeast strains containing the *HIS3* reporter gene under the control of either the *BCCP2* (positive control), *AAD1*, *AAD5* or *FAB2* promoter were transformed with either the empty pDEST22 expression vector or with a version of this vector allowing the expression of *WRI1* before being plated on appropriate media to maintain the expression of the vectors (SD-U-W) and to test the activation of the *HIS3* reporter gene (SD-U-W-H). Data presented are representative from the results obtained for five independent colonies. SD, synthetic drop-out medium.
(F) Binding of WRI1 to the proximal upstream region of *FAB2*. Electrophoretic mobility shift assay (EMSA) of a probe covering a region from -800 to -721 upstream from the ATG codon of *FAB2* (see Supplemental Figure 3). LEAFY COTYLEDON2 (LEC2) was used as a negative control. Competition of WRI1 binding was carried out in the presence of 100-, 500-, and 1,000-fold amounts of the unlabeled *ProFAB2* fragment. Position of free probe (open arrowhead) and the shifted bands (closed arrowhead) are indicated.
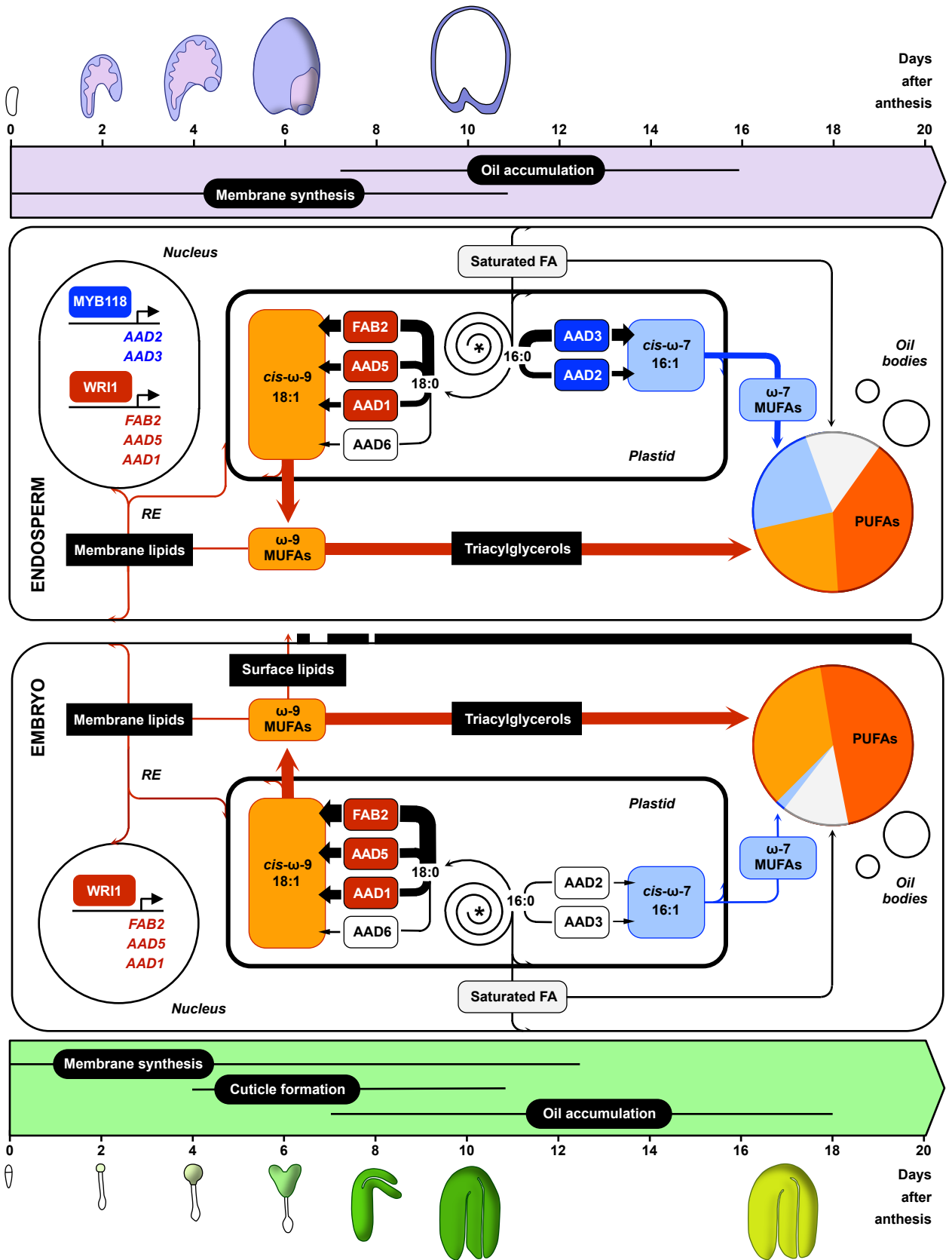
Figure 11. Biosynthesis and fate of monounsaturated fatty acids in developing seeds of *Arabidopsis*.

The WRINKLED1 (WRI1) transcription factor directly enhances the transcription of three Δ9 stearoyl-ACP desaturase (SAD)-coding genes, namely *AAD1*, *AAD5*, and *FAB2*, in zygotic tissues of early-maturing seeds. Endosperm-specific induction of *AAD2* and *AAD3*, that encode Δ9 palmitoyl-ACP desaturases (PADs), is triggered by MYB118 and, to a lesser extent, by MYB115 (not presented). In the developing embryo, ω-9 monounsaturated fatty acids (MUFAs) are essential for the elaboration of membrane lipids, surface lipids, and storage lipids (triacyglycerols). The cuticle deposited at the surface of the embryo, together with the embryo sheath, plays a key role in embryo-endosperm separation and correct embryo elongation during early-maturation. Triacylglycerols stored in the embryo during the maturation phase comprise up to 85 mol % of ω-9 MUFAs and their polyunsaturated derivatives (PUFAs). In the endosperm, ω-9 MUFAs are used for the production of membrane lipids and storage lipids. Due to the concomitant transcriptional activation of SAD- and PAD-coding genes in the maturing endosperm, triacyglycerols accumulated in this seed compartment comprise almost equivalent proportions of ω-7 and ω-9 MUFAs. Recent studies suggest that the cuticle separating endosperm cells from the inner cell layer of the seed coat is of maternal origin (Loubéry et, 2018). The synthesis of this cuticle layer by cells of the seed coat was therefore omitted.

Parsed Citations

Alexander, M.P. (1969). Differential staining of aborted and nonaborted pollen. Stain Technol. 44: 117-122.
Pubmed: Author and Title
Google Scholar: Author Only Title Only Author and Title

Arabidopsis Genome Initiative (2000). Analysis of the genome sequence of the flowering plant Arabidopsis thaliana. Nature 14: 796-815.
Pubmed: Author and Title
Google Scholar: Author Only Title Only Author and Title

Arnold, K., Bordoli, L., Kopp, J., and Schwede, T. (2006). The SWISS-MODEL workspace: a web-based environment for protein structure homology modelling. Bioinformatics 22: 195-201.
Pubmed: Author and Title
Google Scholar: Author Only Title Only Author and Title

Barthole, G., To, A, Marchive, C., Brunaud, V., Soubigou-Taconnat, L., Berger, N., Dubreucq, B., Lepiniec, L., and Baud, S. (2014). MYB118 represses endosperm maturation in seeds of Arabidopsis. Plant Cell 26: 3519-3537.
Pubmed: Author and Title
Google Scholar: Author Only Title Only Author and Title

Bates P.D., Stymne S., and Ohlrogge J. (2013). Biochemical pathways in seed oil synthesis. Curr. Opin. Plant Biol. 16: 1-7.
Pubmed: Author and Title
Google Scholar: Author Only Title Only Author and Title

Baud, S., Boutin, J.P., Miquel, M., Lepiniec, L., and Rochat, C. (2002). An integrated overview of seed development in Arabidopsis thaliana ecotype WS. Plant Physiol. Biochem. 40: 151-160.
Pubmed: Author and Title
Google Scholar: Author Only Title Only Author and Title

Baud, S., Vaultier, M.-N., and Rochat, C. (2004). Structure and expression profile of the sucrose synthase multigene family in Arabidopsis. J. Exp. Bot. 55: 397-409.
Pubmed: Author and Title
Google Scholar: Author Only Title Only Author and Title

Baud, S., Wuillème, S., Dubreucq, B., de Almeida, A, Vuagnat, C., Lepiniec, L., Miquel, M., and Rochat, C. (2007a). Function of plastidial pyruvate kinase in seeds of Arabidopsis thaliana. Plant J. 52: 405-419.
Pubmed: Author and Title
Google Scholar: Author Only Title Only Author and Title

Baud, S., Santos Mendoza, M., To, A, Harscoët, E., Lepiniec, L., and Dubreucq, B. (2007b). WRINKLED1 specifies the regulatory action of LEAFY COTYLEDON2 towards fatty acid metabolism during seed maturation in Arabidopsis. Plant J. 50: 825-838.
Pubmed: Author and Title
Google Scholar: Author Only Title Only Author and Title

Baud, S., Dubreucq, B., Miquel, M., Rochat, C., and lepiniec, L. (2008) Storage reserve accumulation in Arabidopsis: Metabolic and developmental control of seed filling. The Arabidopsis Book 6: 1-24.
Pubmed: Author and Title
Google Scholar: Author Only Title Only Author and Title

Baud, S., Wuillème, S., To, A, Rochat, C., and Lepiniec, L. (2009a). Role of WRINKLED1 in the transcriptional regulation of glycolytic and fatty acid biosynthetic genes in Arabidopsis. Plant J. 60: 933-947.
Pubmed: Author and Title
Google Scholar: Author Only Title Only Author and Title

Baud, S., Reinhard Dichow, N., Kelemen, Z, d'Andréa, S., To, A, Berger, N., Canonge, M., Kronenberger, J., Viterbo, D., Dubreucq, B., Lepiniec, L., Chardot, T., and Miquel, M. (2009b) Regulation of HSD1 in seeds of Arabidopsis thaliana. Plant Cell Physiol. 50: 1463-1478.
Pubmed: Author and Title
Google Scholar: Author Only Title Only Author and Title

Baud, S., and Lepiniec, L. (2010). Physiological and developmental regulation of seed oil production. Prog. Lipid Res. 49: 235-249.
Pubmed: Author and Title
Google Scholar: Author Only Title Only Author and Title

Baud, S., Feria Bourrellier, A.B., Azzopardi, M., Berger, A, Dechorgnat, J., Daniel-Vedele, F., Lepiniec, L., Miquel, M., Rochat, C., Hodges, M., and Ferrario-Méry, S. (2010). PII is induced by WRINKLED1 and fine-tunes fatty acid composition in seeds of Arabidopsis thaliana. Plant J. 64: 291-303.
Pubmed: Author and Title
Google Scholar: Author Only Title Only Author and Title

Bechtold, N., Ellis, J., and Pelletier, G. (1993). In planta infiltration of adult Arabidopsis plants. C. R. Acad. Sci. Paris Life Sci. 316: 1194-1199.
Pubmed: Author and Title
Google Scholar: Author Only Title Only Author and Title

Beeckman, T., De Rycke, R., Viane, R., and Inze, D. (2000). Histological study of seed coat development in Arabidopsis thaliana. J. Plant Res. 113: 139-148.

Pubmed: Author and Title
Google Scholar: Author Only Title Only Author and Title

Belcram, K., Palauqui, J.-C., and Pastuglia, M. (2016). Studying cell division plane positioning in early-stage embryos. Methods Mol. Biol. 1370: 183-195.

Pubmed: Author and Title
Google Scholar: Author Only Title Only Author and Title

Belmonte, M.F., Kirkbride, R.C., Stone, S.L., Pelletier, J.M., Bui, A.Q., Yeung, E.C., Hashimoto, M., Fei, J., Harada, C.M., Munoz, M.D., Le, B.H., Drews, G.N., Brady, S.M., Goldberg, R.B., and Harada, J.J. (2013). Comprehensive developmental profiles of gene activity in regions and subregions of the Arabidopsis seed. Proc. Natl Acad. Sci. USA 110: 435-444.

Pubmed: Author and Title
Google Scholar: Author Only Title Only Author and Title

Bewley, J.D. (1997). Seed germination and dormancy. Plant Cell 9: 1055-1066.

Pubmed: Author and Title
Google Scholar: Author Only Title Only Author and Title

Bordoli, L., Kiefer, F., Arnold, K., Benkert, P., Battey, J., and Schwede, T. (2009). Protein structure homology modelling using SWISS-MODEL workspace. Nat. Protoc. 4: 1-13.

Pubmed: Author and Title
Google Scholar: Author Only Title Only Author and Title

Bryant, F.M., Munoz-Azcarate, O., Kelly, A.A., Beaudoin, F., Kurup, S., and Eastmond, P.J. (2016). ACYL-ACYL CARRIER PROTEIN DESATURASE2 and 3 are responsible for making omega-7 fatty acids in the Arabidopsis aleurone. Plant Physiol. 172: 154-162.

Pubmed: Author and Title
Google Scholar: Author Only Title Only Author and Title

Buda, G.J., Isaacson, T., Matas, A.J., Paolillo, D.J., and Rose, J.K. (2009). Three-dimensional imaging of plant cuticle architecture using confocal scanning laser microscopy. Plant J. 60:378-385.

Pubmed: Author and Title
Google Scholar: Author Only Title Only Author and Title

Cahoon, E.B., Shah, S., Shanklin, J., and Browse, J. (1998). A determinant of substrate specificity predicted from the acyl-acyl carrier protein desaturase of developing cat's claw seed. Plant Physiol. 117: 593-598.

Pubmed: Author and Title
Google Scholar: Author Only Title Only Author and Title

Candela, H., Pérez-Pérez, J.M., and Micol J.L. (2011). Uncovering the post-embryonic functions of gametophytic- and embryonic-lethal genes. Trends Plant Sci. 16: 336-345.

Pubmed: Author and Title
Google Scholar: Author Only Title Only Author and Title

Cao, Y., Xian, M., Yang, J., Xu, X., Liu, W., and Li, L. (2010). Heterologous expression of stearoyl-acyl carrier protein desaturase (S-ACP-DES) from Arabidopsis thaliana in Escherichia coli. Protein Expr. Purif. 69: 209-214.

Pubmed: Author and Title
Google Scholar: Author Only Title Only Author and Title

Cernac, A, and Benning, C. (2004). WRINKLED1 encodes an AP2/EREB domain protein involved in the control of storage compound biosynthesis in Arabidopsis. Plant J. 40: 575-585.

Pubmed: Author and Title
Google Scholar: Author Only Title Only Author and Title

Clemente, T.E., and Cahoon, E.B. (2009). Soybean oil: genetic approaches for modification of functionality and total content. Plant Physiol. 151: 1030-1040.

Pubmed: Author and Title
Google Scholar: Author Only Title Only Author and Title

Creff, A, Brocard, L., Joubès, J., Taconnat, L., Doll, N.M., Marsollier, A.-C., Pascal, S., Galleti, R., Boeuf, S., Moussu, S., Widiez, T., Domergue, F., and Ingram, G. (2019). A stress-response-related inter-compartmental pathway regulates embryonic cuticle integrity in Arabidopsis. PLoS Genet. 15: e1007847.

Pubmed: Author and Title
Google Scholar: Author Only Title Only Author and Title

Curtis, M., and Grossniklaus, U. (2003). A Gateway TM cloning vector set for high-throughput functional analysis of genes in plants. Plant Physiol. 133: 462-469.

Pubmed: Author and Title
Google Scholar: Author Only Title Only Author and Title

Delude, C., Moussu, S., Joubès, J., Ingram, G., and Domergue, F. (2016). Plant surface lipids and epidermis development. Subcell. Biochem. 86: 287-313.

Pubmed: Author and Title
Google Scholar: Author Only Title Only Author and Title

Doll, N.M., Bovio, S., Gaiti, A, Marsollier, A.-C., Chamot, S., Moussu, S., Widiez, T., and Ingram, G. (2020). The endosperm-derived embryo sheath is an anti-adhesive structure that facilitates cotyledon emergence during germination. Curr. Biol. 30: 909-915.
Pubmed: Author and Title
Google Scholar: Author Only Title Only Author and Title

Domergue, F., Vishwanath, S.J., Joubès, J., Ono, J., Lee, J.A., Bourdon, M., Alhattab, R., Lowe, C., Pascal, S., Lessire, R., and Rowland, O. (2010). Three Arabidopsis fatty acyl-coenzyme A reductases, FAR1, FAR4, and FAR5, generate primary fatty alcohols associated with suberin deposition. Plant Physiol. 153: 1539-1554.
Pubmed: Author and Title
Google Scholar: Author Only Title Only Author and Title

Dubos, C., Le Gourrierec, J., Baudry, A, Huep, G., Lanet, E., Debeaujon, I., Routaboul, J.-M., Alboresi, A, Weisshaar, B., and Lepiniec, L. (2008). MYBL2 is a new regulator of flavonoid biosynthesis in Arabidopsis thaliana. Plant J. 55: 940-953.
Pubmed: Author and Title
Google Scholar: Author Only Title Only Author and Title

Ewald, R., Hoffmann, C., Neuhaus, E., and Bauwe, H. (2013). Two redundant octanoyltransferases and one obligatory lipoyl synthase provide protein-lipoylation autonomy to plastids of Arabidopsis. Plant Biol. 16: 35-42.
Pubmed: Author and Title
Google Scholar: Author Only Title Only Author and Title

Fiume, E., Guyon, V., Remoué, C., Magnani, E., Miquel, M., Grain, D., and Lepiniec, L. (2016). TWS1, a novel small protein, regulates various aspects of seed and plant development. Plant Physiol. 172: 1732-1745.
Pubmed: Author and Title
Google Scholar: Author Only Title Only Author and Title

Gao, Q.-M., Venugopal, S., Navarre, D., and Kachroo, A. (2011). Low oleic acid-derived repression of jasmonic acid-inducible defense responses requires the WRKY50 and WRKY51 proteins. Plant Physiol. 155: 464-476.
Pubmed: Author and Title
Google Scholar: Author Only Title Only Author and Title

Gietz, R.D., and Woods, R.A. (2002). Transformation of yeast by lithium acetate/single-stranded carrier DNA/polyethylene glycol methods. Methods Enzymol. 350: 87-96.
Pubmed: Author and Title
Google Scholar: Author Only Title Only Author and Title

Harwood, J. (1996). Recent advances in the biosynthesis of plant fatty acids. Biochim. Biophys. Acta 1301: 7-56.
Pubmed: Author and Title
Google Scholar: Author Only Title Only Author and Title

Hofmann, F., Schon, M.A., and Nodine, M.D. (2019).The embryonic transcriptome of Arabidopsis thaliana. Plant Reprod. 32:77-91.
Pubmed: Author and Title
Google Scholar: Author Only Title Only Author and Title

Ingram, G., and Nawrath, C. (2017). The roles of cuticle in plant development: organ adhesions and beyond. J. Exp. Bot. 68: 5307-5321.
Pubmed: Author and Title
Google Scholar: Author Only Title Only Author and Title

Jin C., Li D., Gao C., Liu K., Qi S., Duan S., Li Z, Gong J., Wang J., Hai J., and Chen M. (2017). Conserved function of ACYL-ACYL CARRIER PROTEIN DESATURASE5 on seed oil and oleic acid biosynthesis between Arabidopsis and Brassica napus. Front Plant Sci 8: 1319.
Pubmed: Author and Title
Google Scholar: Author Only Title Only Author and Title

Jung, S.H., Kim, R.J., Kim, K.J., Lee, D.H., and Suh, M.C. (2019). Plastidial and mitochondrial malonyl CoA-ACP malonyltransferase is essential for cell division and its overexpression increases storage oil content. Plant Cell Physiol. 60: 1239-1249.
Pubmed: Author and Title
Google Scholar: Author Only Title Only Author and Title

Kachroo, A, Lapchyk, L., Fukushige, H., Hildebrand, D., Klessig, D., and Kachroo, P. (2003). Plastidial fatty acid signaling modulates salicylic acid- and jasmonic acid-mediated defense pathways in the Arabidopsis ssi2 mutant. Plant Cell 15: 2952-2965.
Pubmed: Author and Title
Google Scholar: Author Only Title Only Author and Title

Kachroo, A, Shanklin, J., Whittle, E., Lapchyk, L., Hildebrand, D., and Kachroo, P. (2007). The Arabidopsis stearoyl-acyl carrier protein-desaturase family and the accumulation of leaf isoforms to oleic acid synthesis. Plant Mol. Biol. 63: 257-271.
Pubmed: Author and Title
Google Scholar: Author Only Title Only Author and Title

Kachroo, P., Shanklin, J., Shah, J., Whittle, E.J., and Klessig, F. (2001). A fatty acid desaturase modulates the activation of defense signaling pathways in plants. Proc. Natl Acad. Sci. USA 98: 9448-9453.
Pubmed: Author and Title
Google Scholar: Author Only Title Only Author and Title

Kachroo, P., Venugopal, S.C., Navarre, D.A, Lapchyk, L., and Kachroo, A. (2005). Role of salicylic acid and fatty acid desaturation pathways in ssi2-mediated signaling. Plant Physiol. 139: 1717-1735.
  Pubmed: Author and Title
  Google Scholar: Author Only Title Only Author and Title

Kelemen, Z, Przybyla-Toscano, J., Tissot, N., Lepiniec, L., and Dubos, C. (2016). Fast and efficient cloning of Cis-regulatory sequences for high-throughput yeast one-hybrid analyses of transcription factors. Methods Mol. Biol. 1482: 139-149.
  Pubmed: Author and Title
  Google Scholar: Author Only Title Only Author and Title

Kim M.J., Jang I.-C., and Chua N.-H. (2016). The mediator complex MED15 subunit mediates activation of downstream lipid-related genes by the WRINKLED1 transcription factor. Plant Physiol. 171:1951-1964.
  Pubmed: Author and Title
  Google Scholar: Author Only Title Only Author and Title

Klinkenberg, J., Faist, H., Saupe S., Lambertz, S., Krischke, M., Stingl, N., Fekete, A, Mueller, M.J., Feussner, I., Hedrich, R., and Deeken, R. (2014). two fatty acid desaturases, STEAROYL-ACYL CARRIER PROTEIN (9-DESATURASES6 and FATTY ACID DESATURASE3, are involved in drought and hypoxia stress signaling in Arabidopsis crown galls. Plant Physiol. 164: 570-583.
  Pubmed: Author and Title
  Google Scholar: Author Only Title Only Author and Title

Lakhssassi, N., Colantonio, V., Flowers, N.D., Zhou, Z, Henry, J., Liu, S., and Meksem, K. (2017). Stearoyl-acyl carrier protein desaturases mutations unconver an impact of stearic acid in leaf and nodule structure. Plant Physiol. 174: 1531-1543.
  Pubmed: Author and Title
  Google Scholar: Author Only Title Only Author and Title

Laux, T., and Jürgens, G. (1997) Embryogenesis: A new start in life. Plant Cell 9: 989-1000.
  Pubmed: Author and Title
  Google Scholar: Author Only Title Only Author and Title

Le, B.H., Cheng, C., Bui, A.Q., Wagmaister, J.A, Henry, K., Pelletier, J., Kwong, L., Belmonte, M., Kirkbride, R., Horvath, S., Drews, G.N., Fischer, R.L., Okamuro, J.K., Harada, J.J., and Goldberg, R.B. (2010). Global analysis of gene activity during Arabidopsis seed development and identification of seed-specific transcription factors. Proc. Natl. Acad.Sci. USA 107: 8063-8070.
  Pubmed: Author and Title
  Google Scholar: Author Only Title Only Author and Title

Lepiniec, L., Devic, M., Roscoe, T.J., Bouyer, D., Zhou, D.-X., Boulard, C., Baud, S., and Dubreucq, B. (2018) Molecular and epigenetic regulations and functions of the LAFL transcriptional regulators that control seed development. Plant Reprod. 31: 291-307.
  Pubmed: Author and Title
  Google Scholar: Author Only Title Only Author and Title

Li, Y., Beisson, F., and Ohlrogge, J. (2006). Oil content of Arabidopsis seeds: the influence of seed anatomy, light and plant-to-plant variation. Phytochemistry 67: 904-915.
  Pubmed: Author and Title
  Google Scholar: Author Only Title Only Author and Title

Li, Y., Beisson, F., Koo, A.J.K., Molina, I., Pollard, M., and Ohlrogge, J. (2007). Identification of acyltransferases required for cutin biosynthesis and production of cutin with suberin-like monomers. Proc. Natl Acad. Sci. USA 46: 18339-18344.
  Pubmed: Author and Title
  Google Scholar: Author Only Title Only Author and Title

Lightner, J., Wu, J., and Browse, J. (1994). A mutant of Arabidopsis with increased levels of stearic acid. Plant Physiol. 106: 1443-1451.
  Pubmed: Author and Title
  Google Scholar: Author Only Title Only Author and Title

Lightner, J., Lark, E., James, D., and Browse, J. (1997). Novel mutations affecting leaf stearate content and plant size in Arabidopsis. Theor. Appl. Genet. 94: 975-981.
  Pubmed: Author and Title
  Google Scholar: Author Only Title Only Author and Title

Lin, M., Behal, R., and Oliver, D.J. (2003). Disruption of plE2, the gene coding for the E2 subunit of the plastid pyruvate dehydrogenase complex, in Arabidopsis causes an early embryo lethal phenotype. Plant Mol. Biol. 52: 865-872.
  Pubmed: Author and Title
  Google Scholar: Author Only Title Only Author and Title

Liu, J., Wilson, T.E., Milbrandt, J., and Johnston, M. (1993). Identifying DNA-binding sites and analyzing DNA-binding domains using a yeast selection system. Methods 5: 125-137.
  Pubmed: Author and Title
  Google Scholar: Author Only Title Only Author and Title

Loubéry, S., De Giorgi, J., Utz-Pugin, A, Demonsais, L., and Lopez-Molina, L. (2018). A maternally deposited endosperm cuticle contributes to the physiological defects of transparent testa seeds. Plant Physiol. 177: 1218-1233.
  Pubmed: Author and Title
  Google Scholar: Author Only Title Only Author and Title

Maeo K., Tokuda T., Ayame A., Mitsui N., Kawai T., Tsukogashi H., Ishiguro S., and Nakamura K. (2009). An AP2-type transcription factor, WRINKLED1, of Arabidopsis thaliana binds to the AW-box sequence conserved among proximal upstream regions of genes involved in fatty acid synthesis. Plant J 60: 476-487.

Pubmed: Author and Title
Google Scholar: Author Only Title Only Author and Title

Marchive C., Nikovics K., To A, Lepiniec L., and Baud S. (2014). Transcriptional regulation of fatty acid production in higher plants: Molecular bases and biotechnological outcomes. Eur. J. Lipid Sci. Technol. 116: 1332-1343.

Pubmed: Author and Title
Google Scholar: Author Only Title Only Author and Title

Meinke, D.W. (2019). Genome-wide identification of EMBRYO-DEFECTIVE (EMB) genes required for growth and development in Arabidopsis. New Phytol. 226: 306-325.

Pubmed: Author and Title
Google Scholar: Author Only Title Only Author and Title

Moussu S., Doll N.M., Chamot S., Brocard L., Creff A, Fourquin C., Widiez T., Nimchuk Z.L., and Ingram G. (2017). ZHOUPI and KERBEROS mediate embryo/endosperm separation by promoting the formation of an extracuticular sheath at the embryo surface. Plant Cell 29: 1642-1656.

Pubmed: Author and Title
Google Scholar: Author Only Title Only Author and Title

Nakagawa, T., Kurose, T., Hino, T., Tanaka, K., Kawamukai, M., Niwa, Y., Toyooka, K., Matsuoka, K., Jinbo, T., and Kimura, T. (2007). Development of series of Gateway binary vectors, pGWBs, for realizing efficient construction of fusion genes for plant transformation. J. Biosci. Bioeng. 104: 34-41.

Pubmed: Author and Title
Google Scholar: Author Only Title Only Author and Title

Penfield, S., Rylott, E.L., Gilday, A.D., Graham, S., Larson, T.R., and Graham, I.A. (2004). Reserve mobilization in the Arabidopsis endosperm fuels hypocotyl elongation in the dark, is dependent of abscisic acid, and requires PHOSPHOENOLPYRUVATE CARBOXYKINASE1. Plant Cell 16: 2705-2718.

Pubmed: Author and Title
Google Scholar: Author Only Title Only Author and Title

Pidkowich, M.S., Nguyen, H.T., Heilmann, I., Ischebeck, T., and Shanklin, J. (2007). Modulating seed ß-ketoacyl-acyl carrier protein synthase II converts the composition of a temperate seed oil to that of a palm-like tropical oil. Proc. Natl Acad. Sci. USA 104: 4742-4747.

Pubmed: Author and Title
Google Scholar: Author Only Title Only Author and Title

Porterfield, D.M., Kuang, A, Smith, P.J.S., Crispi, M., and Musgrave, M.E. (1999). Oxygen-depleted zones inside reproductive structures of Brassicaceae: implications for oxygen control of seed development. Can. J. Bot. 77: 1439-1446.

Pubmed: Author and Title
Google Scholar: Author Only Title Only Author and Title

Reece-Hoyes J.S., and Walhout, A.J.M. (2012). Yeast one-hybrid assays: a historical and technical perspective. Methods 57: 441-447.

Pubmed: Author and Title
Google Scholar: Author Only Title Only Author and Title

Ruddle II, P., Whetten, R., Cardinal, A, Upchurch, R.G., and Miranda, L. (2013). Effect of a novel mutation in a Δ9-stearoyl-ACP-desaturase on soybean seed oil composition. Theor. Appl. Genet. 126: 241-249.

Pubmed: Author and Title
Google Scholar: Author Only Title Only Author and Title

Sakai, K., Taconnat, L., Borrega, N., Yansouni, J., Brunaud, V., Paysant-Le Roux, C., Delannoy, E., Martin Magniette, M.-L., Lepiniec, L., Faure, J.D., Balzergue, S., and Dubreucq, B. (2018) .Combining laser-assisted microdissection (LAM) and RNA-seq allows to perform a comprehensive transcriptomic analysis of epidermal cells of Arabidopsis embryo. Plant Methods 14: 10.

Pubmed: Author and Title
Google Scholar: Author Only Title Only Author and Title

Savage, L.J., Imre, K.M., Hall, D.A., and Last, R.L. (2013). Analysis of essential Arabidopsis nuclear genes encoding plastid-targeted proteins. PLoS ONE 8: e73291.

Pubmed: Author and Title
Google Scholar: Author Only Title Only Author and Title

Shamloul, M., Trusa, J., Mett, V., and Yusibov, V. (2014). Optimization and utilization of Agrobacterium-mediated transient protein production in Nicotiana. J. Vis. Exp. 86: 51204.

Pubmed: Author and Title
Google Scholar: Author Only Title Only Author and Title

Shanklin J., and Cahoon E.B. (1998). Desaturation and related modifications of fatty acids. Annu Rev Plant Physiol Plant Mol Biol. 49: 611-641.

Pubmed: Author and Title
Google Scholar: Author Only Title Only Author and Title

Schmid, M., Davison, T.S., Henz, S.R., Pape, U.J., Demar, M., Vingron, M., Scholkopf, B., Weigel, D., and Lohmann, J.U. (2005). A gene expression map of Arabidopsis thaliana development. Nat. Genet. 37: 501-506.
Pubmed: Author and Title
Google Scholar: Author Only Title Only Author and Title

Szczuka, E., and Szczuka, A. (2003). Cuticle fluorescence during embryogenesis of Arabidopsis thaliana (L.) Heynh. Acta Biol. Cracov. Bot. 45: 63-67.
Pubmed: Author and Title
Google Scholar: Author Only Title Only Author and Title

Tanaka, H., Onouchi, H., Kondo, M., Hara-Nishimura, I., Nishimura, M., Machida, C., and Machida, Y. (2001). A subtilisn-like serine protease is required for epidermal surface formation in Arabidopsis embryos and juvenile plants. Development 128: 4681-4689.
Pubmed: Author and Title
Google Scholar: Author Only Title Only Author and Title

Tanaka, T., Tanaka, H., Machida, C., Watanabe, M., and Machida, Y. (2004). A new method for rapid visualization of defects in leaf cuticle reveals five intrinsic patterns of surface defects in Arabidopsis. Plant J. 37: 139-146.
Pubmed: Author and Title
Google Scholar: Author Only Title Only Author and Title

To, A, Joubès, J., Barthole, G., Lécureuil, A, Scagnelli, A, Jasinski, S., Lepiniec, L., and Baud S. (2012). WRINKLED transcription factors orchestrate tissue-specific regulation of fatty acid biosynthesis in Arabidopsis. Plant Cell 24: 5007-5023.
Pubmed: Author and Title
Google Scholar: Author Only Title Only Author and Title

Troncoso-Ponce, M.A, Barthole, G., Tremblais, G., To, A, Miquel, M., Lepiniec, L., and Baud, S. (2016a). Transcriptional activation of two delta-9 palmitoyl-ACP desaturase genes by MYB115 and MYB118 is critical for biosynthesis of omega-7 monounsaturated fatty acids in the endosperm of Arabidopsis seeds. Plant Cell 28: 2666-2682.
Pubmed: Author and Title
Google Scholar: Author Only Title Only Author and Title

Troncoso-Ponce, M.A, Nikovics K., Marchive C., Lepiniec L., and Baud S. (2016b). New insights on the organization and regulation of the fatty acid biosynthetic network in the model higher plant Arabidopsis thaliana. Biochimie 120: 3-8.
Pubmed: Author and Title
Google Scholar: Author Only Title Only Author and Title

Tsuwamoto, R., Fukuoka, H., and Takahata, Y. (2008). GASSHO1 and GASSHO2 encoding a putative leucine-rich repeat transmembrane-type receptor kinase are essential for the normal development of the epidermal surface in Arabidopsis embryos. Plant J. 54: 30-42.
Pubmed: Author and Title
Google Scholar: Author Only Title Only Author and Title

Vicente-Carbajosa, J., and Carbonero, P. (2005). Seed maturation: developing an intrusive phase to accomplish a quiescent state. Int. J. Dev. Biol. 49: 645-651.
Pubmed: Author and Title
Google Scholar: Author Only Title Only Author and Title

Vigeolas, H., van Dongen, J.T., Waldeck, P., Hühn, D., and Geigenberger, P. (2003). Lipid storage metabolism is limited by the prevailing low oxygen concentrations within developing seeds of oilseed rape. Plant Physiol. 133: 2048-2060.
Pubmed: Author and Title
Google Scholar: Author Only Title Only Author and Title

Wu, G.-Z, and Xue, H.-W. (2010). Arabidopsis ß-ketoacyl-[acyl carrier protein] synthase I is crucial for fatty acid synthesis and plays a role in chloroplast division and embryo development. Plant Cell 22: 3726-3744.
Pubmed: Author and Title
Google Scholar: Author Only Title Only Author and Title

Xing Q., Creff A, Waters A, Tanaka H., Goodrich J., and Ingram G.C. (2013). ZHOUPI controls embryonic cuticle formation via a signaling pathway involving the subtilisin protease ABNORMAL LEAF-SHAPE1 and the receptor kinases GASSHO1 and GASSHO2. Development 140: 770-779.
Pubmed: Author and Title
Google Scholar: Author Only Title Only Author and Title

Yephremov, A, Wisman, E., Huijser, P., Huijser, C., Wellesen, K., and Saedler, H. (1999). Characterization of the FIDDLEHEAD gene of Arabidopsis reveals a link between adhesion response and cell differentiation in the epidermis. Plant Cell 11: 2197-2201.
Pubmed: Author and Title
Google Scholar: Author Only Title Only Author and Title